IOP Publishing New J. Phys. 27 (2025) 124511 https://doi.org/10.1088/1367-2630/ae228e

New Journal of Physics
The open access journal at the forefront of physics

Deutsche Physikalische Gesellschaft DPG
IOP Institute of Physics

Published in partnership with: Deutsche Physikalische Gesellschaft and the Institute of Physics

PAPER

Refining ensemble *N*-representability of one-body density matrices from partial information

Julia Liebert[1,2], **Anna O Schouten**[3], **Irma Avdic**[3], **Christian Schilling**[1,2,*] **and David A Mazziotti**[3,*]

[1] Department of Physics, Arnold Sommerfeld Center for Theoretical Physics, Ludwig-Maximilians-Universität München, Theresienstrasse 37, 80333 München, Germany
[2] Munich Center for Quantum Science and Technology (MCQST), Schellingstrasse 4, 80799 München, Germany
[3] Department of Chemistry and The James Franck Institute, The University of Chicago, Chicago, IL 60637, United States of America
[*] Authors to whom any correspondence should be addressed.

E-mail: c.schilling@physik.uni-muenchen.de and damazz@uchicago.edu

Keywords: reduced density matrices, density functional theory, reduced density functional theory, ensemble *N*-representability, excited-state ensembles, excited states

OPEN ACCESS

RECEIVED
11 June 2025

REVISED
10 November 2025

ACCEPTED FOR PUBLICATION
21 November 2025

PUBLISHED
11 December 2025

Abstract

The *N*-representability problem places fundamental constraints on reduced density matrices (RDMs) that originate from physical many-fermion quantum states. Motivated by recent developments in functional theories, we introduce a hierarchy of ensemble one-body *N*-representability problems that incorporate partial knowledge of the one-body RDMs (1RDMs) within an ensemble of *N*-fermion states with fixed weights w_i. Specifically, we propose a systematic relaxation that reduces the refined problem—where full 1RDMs are fixed for certain ensemble elements—to a more tractable form involving only natural occupation number vectors. Remarkably, we show that this relaxed problem is related to a generalization of Horn's problem, enabling an explicit solution by combining its constraints with those of the weighted ensemble *N*-representability conditions. An additional convex relaxation yields a convex polytope that provides physically meaningful restrictions on lattice site occupations in ensemble density functional theory for excited states.

1. Introduction

The *N*-representability problem for reduced density matrices (RDMs) is a fundamental challenge in quantum chemistry and many-body quantum physics, particularly in electronic structure theory [1–12]. While computing an RDM from a known quantum state is straightforward, the inverse problem—determining whether a given RDM corresponds to an actual *N*-particle quantum state—is significantly more difficult. This difficulty is formalized by the Quantum Merlin Arthur completeness of the two-body *N*-representability problem [13, 14]. Even for the one-particle reduced density matrix (1RDM), compatibility with a pure *N*-fermion quantum state imposes spectral constraints that are difficult to compute and scale poorly with system size [6, 7, 10, 11, 15–19]. Nonetheless, *N*-representability constraints play a crucial role in both method development in quantum chemistry [1, 20–27] and in quantum algorithms for correlated systems [28–33].

The one-body *N*-representability problem is especially important in the context of functional theories, where it defines the domain of the universal functional in ground-state reduced density matrix functional theory (RDMFT) [23, 34–57]. A 1RDM is compatible with an ensemble of *N*-fermion quantum states if and only if it satisfies the Pauli exclusion principle and is normalized to the particle number [1, 58]. To extend functional theories to excited states, one generalizes the Rayleigh–Ritz variational principle to mixed states of the form $\Gamma = \sum_i w_i |\Psi_i\rangle\langle\Psi_i|$, where the weights $\boldsymbol{w}$ are fixed [59, 60]. In this setting, the domain of the universal functional in $\boldsymbol{w}$-ensemble RDMFT [61–64] and lattice ensemble density functional theory (DFT) [65–75] is determined by the solution to the $\boldsymbol{w}$-ensemble one-body *N*-representability problem [61, 62, 76, 77], whose refinement through additional physical information is the focus of this work.

In this paper, we show that *partial information* about the ground and/or excited states—specifically their 1RDMs—can be used to significantly refine the set of admissible 1RDMs in ensemble calculations for excited states. Building on the traditional $\boldsymbol{w}$-ensemble framework, in which an ensemble of quantum states contributes with fixed weights w_i, we formulate a refined ensemble one-body N-representability problem that incorporates not only the standard representability constraints but also additional structure imposed by fixing one or more of the 1RDMs associated with selected contributing states, such as the ground state $|\Psi_1\rangle$ and low-lying excited states $|\Psi_i\rangle$.

This formulation generalizes Coleman's classical solution, which determines the conditions under which a given 1RDM is representable by an ensemble of N-fermion states, without assuming any knowledge of the contributing states. In contrast, the refined problem considered here assumes not only that the contributing states have fixed weights w_i, but also that the 1RDMs of some of these states are known. This partial information leads to a strictly smaller and more physically meaningful set of ensemble 1RDMs by imposing more stringent N-representability constraints on the unknown remainder of the ensemble. The resulting framework is particularly relevant in practical excited-state simulations, where contributing states are often computed sequentially and partial one-body information is readily available.

The refined $\boldsymbol{w}$-ensemble one-body N-representability problem is highly complex, largely because its solution depends on the natural orbitals of the fixed 1RDMs. As a result, obtaining a complete solution is generally impractical. To address this challenge, we introduce a systematic relaxation in which the fixed 1RDMs are replaced by their natural occupation number vectors, discarding information about the associated orbitals. The resulting relaxed set is characterized purely by spectral data and can be fully described by combining the solution to a generalized version of Horn's problem [78–80] with the $\boldsymbol{w}$-ensemble N-representability constraints [61, 62, 76, 77]. While this yields a complete solution to the relaxed problem, the number of spectral constraints grows rapidly with system size, limiting its scalability.

To overcome this limitation, we derive an outer approximation that provides a set of system-size independent constraints. These constraints remain effective regardless of the number of particles or the dimensionality of the one-particle Hilbert space, making them particularly valuable for quantum chemical applications where large basis sets are required. The tightness of this approximation depends on the deviation of the natural occupation number vectors from the Hartree–Fock point, and thus reflects the degree of correlation in the corresponding N-fermion quantum states.

This paper is organized as follows. Section 2 introduces the notation and terminology for $\boldsymbol{w}$-ensembles that will be used throughout the paper. Section 3 defines the refined $\boldsymbol{w}$-ensemble one-body N-representability problem and outlines the relaxation strategy that yields a practical characterization of the admissible 1RDMs. In section 4, we derive the system-size independent constraints and examine their implications in molecular systems, focusing on ensembles with weakly and strongly correlated ground states. Finally, section 5 shows how taking the convex hull of the spectral constraints leads to a convex set that also governs the lattice site occupation number vectors in ensemble DFT for excited states.

2. Short recap of *w*-ensembles

In this section, we briefly introduce the notation and key aspects of the $\boldsymbol{w}$-ensemble one-body N-representability problem [61, 62, 76] as used in this work. We then reformulate the problem in terms of probabilistic quantum channels, placing it within the broader context of quantum marginal problems studied in the quantum information community [6, 13, 15, 18, 81–93].

We consider systems of N non-relativistic fermions. The N-fermion Hilbert space, $\mathcal{H}_N$, is defined as the N-fold wedge product of the one-particle Hilbert space $\mathcal{H}_1$, i.e. $\mathcal{H}_N = \wedge^N\mathcal{H}_1$. Throughout this work, we assume $\mathcal{H}_1$ is finite-dimensional. The set of pure quantum states on $\mathcal{H}_N$ is denoted by $\mathcal{P}^N$, and the set of ensemble quantum states, $\mathcal{E}^N$, is the convex hull of the pure states, i.e. $\mathcal{E}^N = \mathrm{conv}(\mathcal{P}^N)$.

The one-particle reduced density operator 1RDM of an N-fermion quantum state $\Gamma \in \mathcal{P}^N, \mathcal{E}^N$ is defined as

$$\gamma \equiv N\mathrm{Tr}_{N-1}\left[\Gamma\right]. \tag{1}$$

Due to the linearity of the partial trace, the set $\mathcal{E}^1_N$ of 1RDMs compatible with ensemble N-fermion states is given by

$$\mathcal{E}^1_N \equiv N\mathrm{Tr}_{N-1}\left[\mathcal{E}^N\right], \tag{2}$$

which is also convex. It is the convex hull of the set $\mathcal{P}_N^1$ of 1RDMs compatible with pure N-fermion states, i.e.

$$\mathcal{E}_N^1 = \mathrm{conv}\left(\mathcal{P}_N^1\right). \tag{3}$$

The 1RDMs in $\mathcal{P}_N^1$ are called pure state one-body N-representable, while the 1RDMs in $\mathcal{E}_N^1$ are referred to as ensemble one-body N-representable. Due to the convexity property in equation (3), the ensemble one-body N-representability problem is also known as the convex (relaxed) one-body N-representability problem, a terminology that we adopt in section 3.

According to Watanabe and Coleman [1, 58], the set $\mathcal{E}_N^1$ of ensemble one-body N-representable 1RDMs is fully characterized by the Pauli exclusion principle and the normalization $\mathrm{Tr}_1[\gamma] = N$. In contrast, the set $\mathcal{P}_N^1$ of pure state one-body N-representable 1RDMs is determined by the generalized Pauli constraints [6, 7, 16, 17, 19, 94, 95].

Clearly, pure states are quantum states with a fixed spectrum $\boldsymbol{w}_0 = (1, 0, \dots)$. The set of N-fermion quantum states with a generic fixed spectrum $\boldsymbol{w}$ is denoted by $\mathcal{E}^N(\boldsymbol{w})$, where $\boldsymbol{w} \in \mathbb{R}^D$ with $1 \geqslant w_1 \geqslant w_2 \geqslant \cdots \geqslant w_D \geqslant$ is a decreasingly ordered vector with $\sum_i w_i = 1$, and $D = \dim(\mathcal{H}_N)$. In general, the set $\mathcal{E}^N(\boldsymbol{w})$ is not convex, as the sum of two states with fixed spectra may result in a state with a different spectrum. Therefore, we also introduce its convex hull [61, 62, 76],

$$\bar{\mathcal{E}}^N(\boldsymbol{w}) \equiv \mathrm{conv}\left(\mathcal{E}^N(\boldsymbol{w})\right). \tag{4}$$

Thus, any $\Gamma \in \bar{\mathcal{E}}^N(\boldsymbol{w})$ can be written as a convex combination $\Gamma = \sum_k p_k \Gamma_k$ with $\Gamma_k = \sum_i w_i |\Psi_i^{(k)}\rangle\langle\Psi_i^{(k)}| \in \mathcal{E}^N(\boldsymbol{w})$ and $p_k \geqslant 0, \sum_k p_k = 1$. Due to this convex decomposition, we can further interpret any state $\Gamma \in \bar{\mathcal{E}}^N(\boldsymbol{w})$ as the final state after the application of a probabilistic unitary quantum channel $\chi(\cdot)$ onto a fixed initial state $\Gamma_{\boldsymbol{w}} \in \mathcal{E}^N(\boldsymbol{w})$ as (recall Uhlmann's theorem [96])

$$\chi(\Gamma_{\boldsymbol{w}}) = \sum_k p_k U_k \Gamma_{\boldsymbol{w}} U_k^\dagger, \tag{5}$$

where U_k are unitary operators on $\mathcal{H}_N$. Therefore, $\bar{\mathcal{E}}^N(\boldsymbol{w})$ in equation (4) can be interpreted as the set of states Γ that result from applying probabilistic unitary quantum channels to a fixed but arbitrary $\Gamma_{\boldsymbol{w}} \in \mathcal{E}^N(\boldsymbol{w})$. In particular, equation (5) provides a quantum information perspective on the concept of convex relaxation of non-convex sets as widely exploited in functional theories such as RDMFT [62, 63, 97, 98].

The set of admissible 1RDMs compatible with an N-fermion state in either $\mathcal{E}^N(\boldsymbol{w})$ or $\bar{\mathcal{E}}^N(\boldsymbol{w})$ is defined as [61, 62]

$$\mathcal{E}_N^1(\boldsymbol{w}) = N\mathrm{Tr}_{N-1}\left[\mathcal{E}^N(\boldsymbol{w})\right], \ \bar{\mathcal{E}}_N^1(\boldsymbol{w}) = N\mathrm{Tr}_{N-1}\left[\bar{\mathcal{E}}^N(\boldsymbol{w})\right]. \tag{6}$$

Furthermore, both sets $\mathcal{E}_N^1(\boldsymbol{w})$ and $\bar{\mathcal{E}}_N^1(\boldsymbol{w})$ of 1RDMs are fully characterized by spectral constraints due to their invariance under one-particle unitary transformations. Specifically, for $\bar{\mathcal{E}}_N^1(\boldsymbol{w})$, the corresponding spectral set

$$\Sigma(\boldsymbol{w}) \equiv \left\{\boldsymbol{\lambda} \,|\, \exists \gamma \in \bar{\mathcal{E}}_N^1(\boldsymbol{w}), \pi \in \mathcal{S}_d : \boldsymbol{\lambda} = \pi\left(\mathrm{spec}^{\downarrow}(\gamma)\right)\right\} \tag{7}$$

is indeed a convex polytope as shown in [61, 62, 76]. Here, $\mathcal{S}_d$ denotes the symmetric group of degree $d = \dim(\mathcal{H}_1)$, and the map $\mathrm{spec}^{\downarrow}(\cdot)$ maps a linear operator on a finite-dimensional Hilbert space to its vector of decreasingly ordered eigenvalues. The hyperplane representation of $\Sigma(\boldsymbol{w})$ led to the $\boldsymbol{w}$-ensemble one-body N-representability constraints, which are more restrictive than the Pauli exclusion principle [61, 62, 76].

3. Refined w-ensemble one-body N-representability problem

In this section, we formally introduce and define the refined $\boldsymbol{w}$-ensemble one-body N-representability problem, exploring its variants in terms of solvability and convexity. This will eventually lead to a purely spectral refined $\boldsymbol{w}$-ensemble one-body N-representability problem which is, however, less stringent than the original problem where the knowledge of the full 1RDMs of states in the $\boldsymbol{w}$-ensemble is assumed. While this section is more mathematical and technically detailed, it provides valuable insights that may enrich the understanding of the constraints. In particular, we highlight connections to matrix theory and discrete geometry via the generalized Horn problem (see section 3.2.1), which plays a fundamental role in solving the refined $\boldsymbol{w}$-ensemble one-body N-representability problem. Readers primarily interested in the constraints themselves may proceed directly to section 4.

3.1. Scientific problem

We consider an N-fermion state of the form $\Gamma = \sum_{i=1}^{D} w_i |\Psi_i\rangle\langle\Psi_i|$, which represents a $\boldsymbol{w}$-ensemble $\{w_i, |\Psi_i\rangle\}$ consisting of fixed probabilities w_i and corresponding pure states $|\Psi_i\rangle$. At this stage, we assume the states $|\Psi_i\rangle$ to be mutually orthogonal, i.e. $\langle\Psi_i|\Psi_j\rangle = 0$ for all $i \neq j$, motivated by the fact that they may represent eigenstates of a physical Hamiltonian. This orthogonality assumption will be relaxed later in our analysis.

In the following, we assume additional partial information about the ensemble beyond the fixed probabilities (also called weights) w_i, namely that the 1RDMs of some states $|\Psi_i\rangle$ are known as well. As a simple example, suppose the 1RDM $\gamma^{(1)}$ of a non-degenerate eigenstate $|\Psi_1\rangle$ is known *a priori*. Within the framework of the so-called ensemble variational principle introduced by Gross *et al* [59] (see also [60, 99]), $\gamma^{(1)}$ corresponds to the ground state $|\Psi_1\rangle$ of H. This situation arises, for instance, when $\gamma^{(1)}$ is obtained from a prior ground state calculation, and the ensemble variational principle is then used to determine additional low-lying eigenenergies of H. The constraint imposed by $\gamma^{(1)}$ introduces additional restrictions on the sets $\mathcal{E}^N(\boldsymbol{w})$ and $\mathcal{E}^1_N(\boldsymbol{w})$, which we investigate in this paper.

For the general case of a generic number of known 1RDMs $\gamma^{(i)}$ of states $|\Psi_i\rangle$ in the $\boldsymbol{w}$-ensemble $\{w_i, |\Psi_i\rangle\}$, we introduce the index set K as the set of increasingly ordered indices i that label the fixed 1RDMs $\gamma^{(i)}$. By definition, the set K has cardinality $|K| \leqslant r$, with $i \in \mathbb{N}\backslash 0$ and $1 \leqslant i \leqslant r$ for all $i \in K$. To keep track of these fixed 1RDMs, we define the tuple

$$\mathcal{K}_{\mathrm{K}} \equiv \left(\gamma^{(i)}\right)_{i\in K}, \quad |K| \leqslant r, \tag{8}$$

which contains the 1RDMs $\gamma^{(i)}$ that have been fixed. To assign each index $i \in K$ with the corresponding fixed 1RDM $\gamma^{(i)}$, we introduce (on a technical level) the map

$$\mu : K \to \{1, 2, \ldots, |K|\}\,. \tag{9}$$

In particular, this will allow us in the following to write $\gamma^{(i)} = (\mathcal{K}_{\mathrm{K}})_{\mu(i)}$.

The knowledge of $\mathcal{K}_{\mathrm{K}}$ in equation (8) then implies that the (non-convex) set $\mathcal{E}^N(\boldsymbol{w})$ is restricted to the subset

$$\mathcal{E}^N(\boldsymbol{w}, \mathcal{K}_{\mathrm{K}}) \equiv \left\{\Gamma \in \mathcal{E}^N(\boldsymbol{w}) \,|\forall i \in K\colon |\Psi_i\rangle \mapsto \gamma^{(i)}\right\}, \tag{10}$$

where the map $|\Psi_i\rangle \mapsto \gamma^{(i)}$ is understood as the partial trace map $\gamma^{(i)} = N\mathrm{Tr}_{N-1}[|\Psi_i\rangle\langle\Psi_i|]$.

The corresponding set of 1RDMs γ that are compatible with an N-fermion state $\Gamma \in \mathcal{E}^N(\boldsymbol{w}, \mathcal{K}_{\mathrm{K}})$,

$$\mathcal{E}^1_N(\boldsymbol{w}, \mathcal{K}_{\mathrm{K}}) \equiv N\mathrm{Tr}_{N-1}\left[\mathcal{E}^N(\boldsymbol{w}, \mathcal{K}_{\mathrm{K}})\right], \tag{11}$$

is neither convex nor is it invariant under unitary transformations on the one-particle Hilbert space $\mathcal{H}_1$. Therefore, the set $\mathcal{E}^1_N(\boldsymbol{w}, \mathcal{K}_{\mathrm{K}})$ is not solely characterized by spectral constraints, unlike $\mathcal{E}^1_N(\boldsymbol{w})$ (see equation (6)), and its natural orbital dependence is generally difficult to determine. In fact, $\mathcal{E}^1_N(\boldsymbol{w})$ includes the set $\mathcal{P}^1_N$ of pure state one-body N-representable 1RDMs as a special case, specifically for $\boldsymbol{w}_0 = (1, 0, \ldots)$. Therefore, characterizing $\mathcal{E}^1_N(\boldsymbol{w})$, and thus $\mathcal{E}^1_N(\boldsymbol{w}, \mathcal{K}_{\mathrm{K}}) \subseteq \mathcal{E}^1_N(\boldsymbol{w})$, is expected to be more complex than calculating the generalized Pauli constraints [6, 7, 94]. As a result, directly characterizing $\mathcal{E}^1_N(\boldsymbol{w}, \mathcal{K}_{\mathrm{K}})$ using refined $\boldsymbol{w}$-ensemble N-representability constraints that account for the knowledge of the 1RDMs in $\mathcal{K}_{\mathrm{K}}$ proves to be highly challenging. To address this difficulty, it becomes necessary to systematically relax the definition of $\mathcal{E}^1_N(\boldsymbol{w}, \mathcal{K}_{\mathrm{K}})$ in equation (11). This relaxation, which we will discuss in detail in the following, gives rise to an outer approximation of the original set.

According to the duality principle for compact convex sets (e.g. see [100]), such sets can be fully characterized by the intersection of their supporting hyperplanes. Moreover, replacing a set with its convex hull does not alter the result of minimizing or maximizing linear functionals over it, as is commonly done when solving the ground state problem in physics and quantum chemistry including RDMFT, except that the optimizer may no longer be unique. Thus, we first introduce the convex hull of $\mathcal{E}^N(\boldsymbol{w}, \mathcal{K}_{\mathrm{K}})$ in (10) at the N-fermion level,

$$\bar{\mathcal{E}}^N(\boldsymbol{w}, \mathcal{K}_{\mathrm{K}}) \equiv \mathrm{conv}\left(\mathcal{E}^N(\boldsymbol{w}, \mathcal{K}_{\mathrm{K}})\right). \tag{12}$$

To get a deeper understanding of the implications of taking the convex hull in equation (12), we note that any $\Gamma \in \bar{\mathcal{E}}^N(\boldsymbol{w}, \mathcal{K}_{\mathrm{K}})$ can be written as a convex combination

$$\Gamma = \sum_j p_j \Gamma_j = \sum_{i=1}^{r} w_i \sum_j p_j |\Psi_i^{(j)}\rangle\langle\Psi_i^{(j)}|, \tag{13}$$

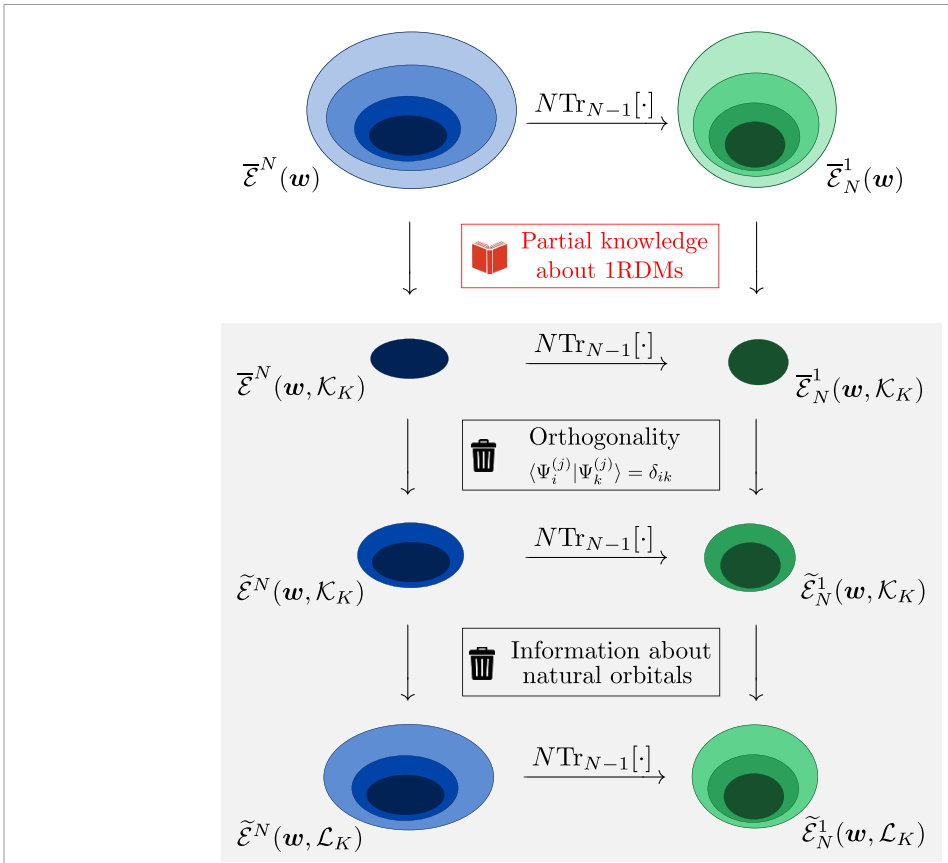

Figure 1. Schematic illustration of the refined $\boldsymbol{w}$-ensemble N-representability problem and its systematic relaxations employed in the text. The gray-shaded area is the scope of this paper. At the N-fermion level (left column) and the one-particle level (right column) the sets $\bar{\mathcal{E}}^N(\boldsymbol{w},\mathcal{K}_\mathrm{K})$ and $\bar{\mathcal{E}}^1_N(\boldsymbol{w},\mathcal{K}_\mathrm{K})$ are obtained from $\bar{\mathcal{E}}^N(\boldsymbol{w})$ and $\bar{\mathcal{E}}^1_N(\boldsymbol{w})$ described in [61, 62, 76] by exploiting partial information about selected 1RDMs of the $\boldsymbol{w}$-ensemble. The figure also indicates a sequence of systematic relaxations that yield the feasible set $\widetilde{\mathcal{E}}^1_N(\boldsymbol{w},\mathcal{L}_K)$, which we characterize in section 3.2.

where $p_j \geqslant 0$, $\sum_j p_j = 1$, and $\Gamma_j \in \mathcal{E}^N(\boldsymbol{w},\mathcal{K}_\mathrm{K})$ for all j. Thus, the 1RDM of Γ in equation (13) follows from the linearity of the partial trace as

$$\gamma = \sum_{i=1}^{r} w_i \sum_j p_j \gamma_j^{(i)} \tag{14}$$

with $\gamma_j^{(i)} \equiv N\mathrm{Tr}_{N-1}[|\Psi_i^{(j)}\rangle\langle\Psi_i^{(j)}|]$. For the indices $i \in K$ (equivalently, $\gamma^{(i)} = (\mathcal{K}_\mathrm{K})_{\mu(i)}$), $\gamma_j^{(i)} = \gamma_{j'}^{(i)}$ for-all j, j' such that the 1RDMs associated with $w_i, i \in K$ in the summation in equation (13) remain unchanged. For completeness, we note that this property of the set in equation (12) with respect to the 1RDMs $\gamma^{(i)} = (\mathcal{K}_\mathrm{K})_{\mu(i)}$ can also be expressed using the probabilistic quantum channel perspective based on equation (5).

At the one-particle level, the set $\bar{\mathcal{E}}^1_N(\boldsymbol{w},\mathcal{K}_\mathrm{K})$ of 1RDMs compatible with a state $\Gamma \in \bar{\mathcal{E}}^N(\boldsymbol{w},\mathcal{K}_\mathrm{K})$ is given by

$$\bar{\mathcal{E}}^1_N(\boldsymbol{w},\mathcal{K}_\mathrm{K}) = \mathrm{conv}\left(\mathcal{E}^1_N(\boldsymbol{w},\mathcal{K}_\mathrm{K})\right). \tag{15}$$

Since the 1RDMs $\gamma^{(i)} = (\mathcal{K}_\mathrm{K})_{\mu(i)}$ are fixed, the set $\bar{\mathcal{E}}^1_N(\boldsymbol{w},\mathcal{K}_\mathrm{K})$ remains non-unitarily invariant and cannot be fully characterized by spectral constraints. In particular, its dependence on the natural orbitals becomes highly complex when multiple 1RDMs $\gamma^{(i)}$ with different natural orbital bases are fixed.

Figure 1 provides an overview that summarizes the key concepts and relaxations discussed in this section after convex relaxation (gray shaded area). The additional sets shown in figure 1 are introduced and explained below. In particular, $\bar{\mathcal{E}}^1_N(\boldsymbol{w},\mathcal{K}_\mathrm{K})$ and $\bar{\mathcal{E}}^N(\boldsymbol{w},\mathcal{K}_\mathrm{K})$ (second row), obtained by incorporating partial information from selected 1RDMs in the $\boldsymbol{w}$-ensemble, serve as the starting point for the following discussion.

To make the problem more tractable, it is necessary to relax the orthonormality condition $\langle\Psi_i^{(j)}|\Psi_k^{(j)}\rangle = \delta_{ik}$, which must hold for all $i \in \{1,\dots,r\}$ in equation (13), for the states $|\Psi_i^{(j)}\rangle$ that correspond to fixed 1RDMs $\gamma^{(i)} \in \mathcal{K}_{\mathrm{K}}$. On the N-fermion level, this leads to the set (see third row in figure 1)

$$\widetilde{\mathcal{E}}^N(\boldsymbol{w},\mathcal{K}_{\mathrm{K}}) \equiv \left\{\Gamma \in \mathcal{E}^N \,\middle|\, \Gamma = \sum_{i\in K} w_i\Gamma^{(i)} + \widetilde{\Gamma}, \Gamma^{(i)} \mapsto (\mathcal{K}_{\mathrm{K}})_{\mu(i)}, \widetilde{\Gamma} \in \bar{\mathcal{E}}^N(\boldsymbol{w}_{K^c})\right\}, \tag{16}$$

where we defined the complement $K^c = J\backslash K$ of the index set K on the index set $J = \{1,2,\dots,r\}$, $\boldsymbol{w}_{K^c} \in \mathbb{R}^{D-|K|}$ is the decreasingly ordered vector of weights w_i that correspond to non-fixed $\gamma^{(i)}$, and

$$\bar{\mathcal{E}}^N(\boldsymbol{w}_{K^c}) \equiv \left\{\Gamma = \sum_j p_j \sum_{i\in K^c} w_i |\Psi_i^{(j)}\rangle\langle\Psi_i^{(j)}| \,\middle|\, \forall i,k \in K^c : \langle\Psi_i^{(j)}|\Psi_k^{(j)}\rangle = \delta_{ik}\right\}. \tag{17}$$

Furthermore, the set of 1RDMs compatible with an N-fermion density operator $\Gamma \in \widetilde{\mathcal{E}}^N(\boldsymbol{w},\mathcal{K}_{\mathrm{K}})$ is given by

$$\widetilde{\mathcal{E}}_N^1(\boldsymbol{w},\mathcal{K}_{\mathrm{K}}) \equiv N\mathrm{Tr}_{N-1}\left[\widetilde{\mathcal{E}}^N(\boldsymbol{w},\mathcal{K}_{\mathrm{K}})\right]. \tag{18}$$

Since $\gamma^{(i)} = (\mathcal{K}_{\mathrm{K}})_{\mu(i)}$, we can equivalently characterize the above set as

$$\widetilde{\mathcal{E}}_N^1(\boldsymbol{w},\mathcal{K}_{\mathrm{K}}) = \left\{\gamma = \sum_{i\in K} w_i\gamma^{(i)} + \widetilde{\gamma} \,\middle|\, \widetilde{\gamma} \in \bar{\mathcal{E}}_N^1(\boldsymbol{w}_{K^c})\right\}, \tag{19}$$

where

$$\bar{\mathcal{E}}_N^1(\boldsymbol{w}_{K^c}) \equiv N\mathrm{Tr}_{N-1}\left[\bar{\mathcal{E}}^N(\boldsymbol{w}_{K^c})\right] \tag{20}$$

is the set of 1RDMs compatible with a linear operator in $\bar{\mathcal{E}}^N(\boldsymbol{w}_{K^c})$.

By construction, the set $\widetilde{\mathcal{E}}_N^1(\boldsymbol{w},\mathcal{K}_{\mathrm{K}})$ (19) satisfies the inclusion relation

$$\bar{\mathcal{E}}_N^1(\boldsymbol{w},\mathcal{K}_{\mathrm{K}}) \subseteq \widetilde{\mathcal{E}}_N^1(\boldsymbol{w},\mathcal{K}_{\mathrm{K}}), \tag{21}$$

as we merely relaxed the condition on 1RDMs γ to be in the set $\bar{\mathcal{E}}_N^1(\boldsymbol{w},\mathcal{K}_{\mathrm{K}})$ compared to $\widetilde{\mathcal{E}}_N^1(\boldsymbol{w},\mathcal{K}_{\mathrm{K}})$. The inclusion relation in equation (21) extends to the N-fermion level and is illustrated at both N-particle and one-particle level in figure 1. Furthermore, the set $\widetilde{\mathcal{E}}_N^1(\boldsymbol{w},\mathcal{K}_{\mathrm{K}})$ is convex, as it follows from the convexity of $\widetilde{\mathcal{E}}^N(\boldsymbol{w},\mathcal{K}_{\mathrm{K}})$, which can be readily proven, and the linearity of the partial trace map $N\mathrm{Tr}_{N-1}[\cdot]$.

To illustrate why the set $\widetilde{\mathcal{E}}_N^1(\boldsymbol{w},\mathcal{K}_{\mathrm{K}})$ as an outer approximation to $\bar{\mathcal{E}}_N^1(\boldsymbol{w},\mathcal{K}_{\mathrm{K}})$ is easier to characterize than the original set $\bar{\mathcal{E}}_N^1(\boldsymbol{w},\mathcal{K}_{\mathrm{K}})$, we consider the case of $r=2$ with $|K|=1$, and we fix $\gamma^{(1)}$. The analysis for $\gamma^{(2)}$ fixed follows analogously. Then, given a 1RDM γ, we have $\gamma \in \widetilde{\mathcal{E}}_N^1(\boldsymbol{w},\gamma^{(1)})$ if and only if $\gamma \in \bar{\mathcal{E}}_N^1(\boldsymbol{w})$ and

$$\gamma^{(2)} = \frac{1}{1-w}\left(\gamma - w\gamma^{(1)}\right) \in \mathcal{E}_N^1. \tag{22}$$

We observe that $\gamma^{(2)}$ is not well-defined, as $w \to 1$, consistent with $\boldsymbol{w}_0 = (1,0,\dots)$ representing an ensemble containing only ground state information and no excited state contributions. Both memberships $\gamma \in \bar{\mathcal{E}}_N^1(\boldsymbol{w})$ and $\gamma^{(2)} \in \mathcal{E}_N^1$ can be verified solely by evaluating spectral constraints, as detailed in [61, 62, 76]. Thus, for $r=2$, we obtain a practical approximation of the more intricate set $\bar{\mathcal{E}}_N^1(\boldsymbol{w},\gamma^{(1)})$.

For general $r \geqslant 3$, however, determining a feasible characterization of the set $\widetilde{\mathcal{E}}_N^1(\boldsymbol{w},\mathcal{K}_{\mathrm{K}})$ remains challenging. To obtain a set of 1RDMs defined solely through spectral constraints, we must discard information about the natural orbitals of the fixed 1RDMs in $\mathcal{K}_{\mathrm{K}}$, retaining only their natural occupation number vectors $\boldsymbol{\lambda}^{(i)} = \pi(\mathrm{spec}^{\downarrow}(\gamma^{(i)})), \pi \in \mathcal{S}_d$, where $d = \dim(\mathcal{H}_1)$. This eventually leads to the last row in figure 1.

3.2. Discarding information about natural orbitals

In this section, we show that discarding information about the natural orbital bases of $\gamma^{(i)} = (\mathcal{K}_{\mathrm{K}})_{\mu(i)}$ allows for a complete characterization of the accordingly relaxed set $\widetilde{\mathcal{E}}^1_N(\boldsymbol{w}, \mathcal{K}_{\mathrm{K}})$ (19) by combining the solution to Horn's problem [78, 80] with the $\boldsymbol{w}$-ensemble one-body N-representability constraints [61, 62, 76].

Neglecting the information about the natural orbitals of the 1RDMs in $\mathcal{K}_{\mathrm{K}}$ and retaining only their spectral information implies considering the tuple

$$\mathcal{L}_K \equiv \left(\boldsymbol{\lambda}^{(i)}\right)_{i\in K} \tag{23}$$

of fixed natural occupation number vectors $\boldsymbol{\lambda}^{(i)}$, similarly to $\mathcal{K}_{\mathrm{K}}$ in equation (8). Using $\mathcal{L}_K$ (23), the set of admissible 1RDMs under this constraint is given by

$$\widetilde{\mathcal{E}}^1_N(\boldsymbol{w}, \mathcal{L}_K) \equiv \bigcup_{u_1,\ldots,u_{|K|}\in \mathrm{U}(\mathcal{H}_1)} \widetilde{\mathcal{E}}^1_N\left(\boldsymbol{w}, \left(u_i D\left(\boldsymbol{\lambda}^{(i)}\right) u_i^\dagger\right)_{i\in K}\right), \tag{24}$$

where $\mathrm{U}(\mathcal{H}_1)$ is the group of unitary operators on $\mathcal{H}_1$, and $D(\boldsymbol{\lambda}^{(i)})$ denotes the diagonal matrix with matrix elements $D_{ij} = \delta_{ij}\lambda^{(i)}_j$. In particular, $\widetilde{\mathcal{E}}^1_N(\boldsymbol{w}, \mathcal{L}_K)$ satisfies the inclusion relation (recall equation (21))

$$\bar{\mathcal{E}}^1_N(\boldsymbol{w}, \mathcal{K}_{\mathrm{K}}) \subseteq \widetilde{\mathcal{E}}^1_N(\boldsymbol{w}, \mathcal{K}_{\mathrm{K}}) \subseteq \widetilde{\mathcal{E}}^1_N(\boldsymbol{w}, \mathcal{L}_K)\,. \tag{25}$$

Both $\widetilde{\mathcal{E}}^1_N(\boldsymbol{w}, \mathcal{L}_K)$ and its preimage $\widetilde{\mathcal{E}}^N(\boldsymbol{w}, \mathcal{L}_K)$ under the partial trace map $N\mathrm{Tr}_{N-1}[\cdot]$ at the N-fermion level are illustrated in figure 1. The figure also shows the inclusion relations among the three sets in equation (25) and their N-fermion counterparts.

The set $\widetilde{\mathcal{E}}^1_N(\boldsymbol{w}, \mathcal{L}_K)$ is eventually invariant under unitary transformations on the one-particle Hilbert space, meaning that for all 1RDMs γ and one-particle unitaries $u : \mathcal{H}_1 \to \mathcal{H}_1$, $\gamma \in \widetilde{\mathcal{E}}^1_N(\boldsymbol{w}, \mathcal{L}_K)$ implies that $u\gamma u^\dagger \in \widetilde{\mathcal{E}}^1_N(\boldsymbol{w}, \mathcal{L}_K)$. This follows directly from the fact that unitary transformations at the one-particle level preserve the spectrum of a 1RDM and that $\mathcal{E}^1_N$ is also unitarily invariant. Consequently, the set $\widetilde{\mathcal{E}}^1_N(\boldsymbol{w}, \mathcal{L}_K)$ in equation (24) is solely characterized by spectral constraints and we denote the corresponding set of admissible spectra by

$$\Lambda\left(\boldsymbol{w}, \mathcal{L}_K\right) \equiv \left\{\boldsymbol{\lambda} \in \mathbb{R}^d \,\middle|\, \exists \gamma \in \widetilde{\mathcal{E}}^1_N(\boldsymbol{w}, \mathcal{L}_K), \pi \in \mathcal{S}_d : \boldsymbol{\lambda} = \pi\left(\mathrm{spec}^{\downarrow}(\gamma)\right)\right\}. \tag{26}$$

Here, we use Λ instead of Σ (cf equation (7)) to emphasize that $\Lambda(\boldsymbol{w}, \mathcal{L}_K)$ is in general *not* a convex polytope for generic $\boldsymbol{\lambda}^{(i)} = (\mathcal{L}_K)_{\mu(i)}, i \in \{1, \ldots, |K|\}$. This can be understood by analogy with the moment polytope described by the generalized Pauli constraints, which is, in general, a convex polytope only for decreasingly ordered natural occupation numbers, but not for the full orbit of this polytope under the action of the symmetric group [6, 7, 15].

It is important to note that the mapping from 1RDMs to their vectors of eigenvalues is inherently non-linear. As a result, the spectrum of a 1RDM $\gamma \in \bar{\mathcal{E}}^1_N(\boldsymbol{w}, \mathcal{K}_{\mathrm{K}})$ cannot, in general, be expressed as a convex combination of the form $\pi(\mathrm{spec}^{\downarrow}(\gamma)) = \sum_{i=1}^r w_i \boldsymbol{\lambda}^{(i)}, \pi \in \mathcal{S}_d$. This non-linearity is a key feature of the spectral problem and highlights the relevance of the generalized Horn's problem [78–80] in this context. In particular, it motivates the connection of Horn's problem to our refined formulation of the one-body N-representability problem, which will be introduced in the next section as a framework for characterizing the set $\Lambda(\boldsymbol{w}, \mathcal{L}_K)$.

3.2.1. Generalized Horn problem

The generalized Horn problem, which deals with the sum of principal submatrices of a Hermitian matrix [80], extends the well-known Horn problem [78, 79, 101, 102] beyond the sum of two Hermitian matrices. Thus, Horn's problem corresponds to the case of $|K| = 1$ fixed natural occupation number vectors (see section 2) and will be used to derive stricter bounds on the residuals of the $\boldsymbol{w}$-ensemble N-representability constraints in section 4, where the residuals are defined as the difference between the right-hand side and the left-hand side of the $\boldsymbol{w}$-ensemble N-representability constraints. Additionally, the generalized Horn problem, with the original Horn problem as a special case, generalizes to settings with an arbitrary cardinality $|K|$ of the set $\mathcal{L}_K$ defined in equation (23).

The generalized Horn problem raises the following question: Given $(m+1)$ decreasingly ordered vectors $\boldsymbol{y}^{\downarrow}, \boldsymbol{x}^{(i)\downarrow} \in \mathbb{R}^d, i \in \{1, \ldots, m\}$, do there exist $(m+1)$ Hermitian matrices $Y, X^{(i)} \in \mathbb{R}^{d\times d}$ such that $Y = \sum_{i=1}^m X^{(i)}$? Here, $\boldsymbol{y}^{\downarrow} = \mathrm{spec}^{\downarrow}(Y)$ and $\boldsymbol{x}^{(i)\downarrow} = \mathrm{spec}^{\downarrow}(X^{(i)})$. Due to the convexity properties of moment

polytopes (e.g. see [103, 104]) the set of admissible $\boldsymbol{y}^{\downarrow}$ for some fixed $\boldsymbol{x}^{(i)\downarrow}, i \in \{1,\ldots,m\}$ is a convex polytope [78, 80, 101, 102]. We denote this set of admissible $\boldsymbol{y}^{\downarrow}$ by $\Sigma_{\mathrm{H}}^{\downarrow}(\{\boldsymbol{x}^{(i)\downarrow}\}_{i=1}^{m})$, where the subscript H stands for Horn's problem. As $\Sigma_{\mathrm{H}}^{\downarrow}(\{\boldsymbol{x}^{(i)\downarrow}\}_{i=1}^{m})$ is a convex polytope, it is characterized by the intersection of finitely many hyperplanes. The corresponding halfspaces describe linear constraints on $\boldsymbol{y}^{\downarrow}$, which strongly depend on d and are highly non-trivial already for the case of three matrices $Y, X^{(1)}, X^{(2)}$ as in the original Horn's problem. For a comprehensive derivation and discussion of the resulting linear constraints, we refer the reader to [78–80, 101, 102].

Due to the Hermiticity of the 1RDM, we observe that the convex combination of 1RDM's

$$\gamma = \sum_{i \in K} w_i \gamma^{(i)} + \widetilde{\gamma} \tag{27}$$

and the individual terms in the above summation relate to the vectors $\boldsymbol{y}, \boldsymbol{x}^{(i)}$ in Horn's problem and its generalization according to $m = |K| + 1$, $Y \equiv \gamma, X^{(i)} = w_{\mu^{-1}(i)} (\mathcal{L}_K)_{\mu(i)}$ for all $i \in \{1,\ldots,|K|\}$ and $X^{(|K|+1)} = \widetilde{\gamma}$, where only $\boldsymbol{x}^{(i)^{\downarrow}} \equiv w_i \boldsymbol{\lambda}^{(i)\downarrow}$ are known *a priori*. This implies to consider the union of the set $\Sigma_{\mathrm{H}}^{\downarrow}(\{w_i \boldsymbol{\lambda}^{(i)\downarrow}\}_{i=1}^{r})$, where $\boldsymbol{\lambda}^{(i)}$ are fixed for all $i \in K$, according to

$$\Lambda_{\mathrm{H}}^{\downarrow}(\boldsymbol{w}, \mathcal{L}_K) \equiv \bigcup_{\boldsymbol{x}^{(|K|+1)\downarrow} \in \Sigma^{\downarrow}(\boldsymbol{w}_{K^c})} \Sigma_{\mathrm{H}}^{\downarrow}\left(\left\{ \boldsymbol{x}^{(i)\downarrow} \right\}_{i=1}^{|K|+1} \right), \tag{28}$$

where $\boldsymbol{w}_0 = (1, 0, \ldots)$ and we defined the set

$$\Sigma^{\downarrow}(\boldsymbol{w}_{K^c}) \equiv \left\{ \boldsymbol{\lambda} \in \mathbb{R}^d \,\middle|\, \exists \gamma \in \bar{\mathcal{E}}_N^1(\boldsymbol{w}_{K^c}) : \boldsymbol{\lambda} = \mathrm{spec}^{\downarrow}(\gamma) \right\}. \tag{29}$$

We use the understanding and characterization of the set $\Lambda_{\mathrm{H}}^{\downarrow}(\boldsymbol{w}, \mathcal{L}_K)$ in equation (28) in the following section to eventually characterize $\Lambda(\boldsymbol{w}, \mathcal{L}_K)$.

3.2.2. Characterization of $\Lambda(\boldsymbol{w}, \mathcal{L}_K)$

In this section, we use the solution to Horn's problem and its generalization for sums of m Hermitian matrices, as discussed in [78–80, 101, 102], to fully characterize $\Lambda(\boldsymbol{w}, \mathcal{L}_K)$ for generic r and cardinality $|K|$ of the index set K. The first key result is the following Lemma:

Lemma 1. *The set*

$$\Lambda^{\downarrow}(\boldsymbol{w}, \mathcal{L}_K) \equiv \left\{ \boldsymbol{\lambda}^{\downarrow} \,\middle|\, \boldsymbol{\lambda} \in \Lambda(\boldsymbol{w}, \mathcal{L}_K) \right\} \tag{30}$$

of decreasingly ordered natural occupation number vectors $\boldsymbol{\lambda}$ *is given by*

$$\Lambda^{\downarrow}(\boldsymbol{w}, \mathcal{L}_K) = \Lambda_{\mathrm{H}}^{\downarrow}(\boldsymbol{w}, \mathcal{L}_K) \cap \Sigma(\boldsymbol{w}). \tag{31}$$

In fact, every 1RDM $\gamma \in \widetilde{\mathcal{E}}_N^1(\boldsymbol{w}, \mathcal{L}_K)$ (24) can be written as a convex combination

$$\gamma = \sum_{i \in K} w_i \gamma^{(i)} + \widetilde{\gamma} \tag{32}$$

for some $\widetilde{\gamma} \in \bar{\mathcal{E}}_N^1(\boldsymbol{w}_{K^c})$. Together with Coleman's ensemble N-representability constraints [1] and the relaxed one-body $\boldsymbol{w}$-ensemble N-representability constraints characterizing $\Sigma(\boldsymbol{w})$ [61, 62, 76], this yields the right-hand side of equation (31).

The union of convex sets, as in the definition of $\Lambda_{\mathrm{H}}^{\downarrow}(\boldsymbol{w}, \mathcal{L}_K)$ in equation (28), and its intersection with a convex set, is generally not convex. Thus, it is essential to demonstrate that the set $\Lambda^{\downarrow}(\boldsymbol{w}, \mathcal{L}_K)$ indeed satisfies:

Theorem 2. *The set* $\Lambda^{\downarrow}(\boldsymbol{w}, \mathcal{L}_K)$ *is a convex polytope.*

Proof. We first prove that $\Lambda_{\mathrm{H}}^{\downarrow}(\boldsymbol{w}, \mathcal{L}_K)$ as defined in equation (28) is convex. Since $\Sigma_{\mathrm{H}}^{\downarrow}(\{\boldsymbol{x}^{(i)\downarrow}\}_{i=1}^{|K|+1})$ is a convex polytope for any choice of $\boldsymbol{x}^{(|K|+1)\downarrow} \equiv \widetilde{\boldsymbol{\lambda}}^{\downarrow} \in \Sigma^{\downarrow}(\boldsymbol{w}_{K^c})$, it is characterized by

$$A \cdot \boldsymbol{\lambda}^{\downarrow} \leqslant C \cdot \widetilde{\boldsymbol{\lambda}}^{\downarrow} + \sum_{i \in K} w_i B_i \cdot \boldsymbol{\lambda}^{(i)\downarrow}, \tag{33}$$

where A, B_i and C are coefficient matrices. The explicit A, B_i, C are dependent on $r, |K|, d$ and follow from the solution to the principal submatrix problem for Hermitian matrices in [80].

Then, for any pair of $\boldsymbol{\lambda}, \boldsymbol{\lambda}' \in \Lambda_{\mathrm{H}}^{\downarrow}(\boldsymbol{w}, \mathcal{L}_K)$ there exist respective $\widetilde{\boldsymbol{\lambda}}^{\downarrow}, \widetilde{\boldsymbol{\lambda}}'^{\downarrow} \in \Sigma(\boldsymbol{w}_{K^c})$ such that $\boldsymbol{\lambda}, \boldsymbol{\lambda}'$ are in the respective polytope $\Sigma_{\mathrm{H}}^{\downarrow}(\{\boldsymbol{x}^{(i)\downarrow}\}_{i=1}^{|K|+1})$ (recall equation (28)). The convexity of the set $\Sigma(\boldsymbol{w}_{K^c})$ in equation (29) then implies that for any $\alpha \in [0,1]$,

$$\alpha\boldsymbol{\lambda} + (1-\alpha)\,\boldsymbol{\lambda}' \in \Lambda_{\mathrm{H}}^{\downarrow}(\boldsymbol{w}, \mathcal{L}_K)\,. \tag{34}$$

Thus, $\Lambda_{\mathrm{H}}^{\downarrow}(\boldsymbol{w}, \mathcal{L}_K)$ is convex. Since the spectral polytope $\Sigma(\boldsymbol{w})$ in equation (7) is convex, also its intersection with the set $\Lambda_{\mathrm{H}}^{\downarrow}(\boldsymbol{w}, \mathcal{L}_K)$ is convex. As both $\Sigma(\boldsymbol{w})$ and $\Lambda_{\mathrm{H}}^{\downarrow}(\boldsymbol{w}, \mathcal{L}_K)$ are not only convex but convex polytopes, also $\Lambda^{\downarrow}(\boldsymbol{w}, \mathcal{L}_K)$ is a convex polytope. □

Therefore, the characterization of the $\Lambda^{\downarrow}(\boldsymbol{w}, \mathcal{L}_K)$ in equation (26) relies on the solution to the generalized Horn problem discussed in section 3.2.1. These constraints, provided in [80], apply to a general number $|K|+1$ of matrices in the weighted sums on the right-hand side of equation (32). The steps to obtain the set $\Lambda(\boldsymbol{w}, \mathcal{L}_K)$, which will be discussed and illustrated in more detail below, are summarized in the following protocol:

Schematic algorithm for calculating $\Lambda(\boldsymbol{w}, \mathcal{L}_K)$

(i) Calculate $\Lambda_{\mathrm{H}}^{\downarrow}(\boldsymbol{w}, \mathcal{L}_K)$ in equation (28) using lemma 2.1 of [80] and $\Sigma^{\downarrow}(\boldsymbol{w}_{K^c})$ obtained from [61, 62, 76].
(ii) Apply lemma 1 to obtain $\Lambda^{\downarrow}(\boldsymbol{w}, \mathcal{L}_K)$ either by collecting the inequalities of the hyperplane representations of $\Sigma(\boldsymbol{w})$ and $\Lambda_{\mathrm{H}}^{\downarrow}(\boldsymbol{w}, \mathcal{L}_K)$, or by explicitly calculating their intersection (e.g. using SAGEMATH [105]).
(iii) *(Optional)* Determine a non-redundant hyperplane representation of $\Lambda^{\downarrow}(\boldsymbol{w}, \mathcal{L}_K)$.
(iv) Calculate $\Lambda(\boldsymbol{w}, \mathcal{L}_K)$ as the orbit of $\Lambda^{\downarrow}(\boldsymbol{w}, \mathcal{L}_K)$ under the action of the symmetric group $\mathcal{S}_d$ of degree d.

By lemma 1 and theorem 2, a (generally non-minimal) hyperplane representation of $\Lambda^{\downarrow}(\boldsymbol{w}, \mathcal{L}_K)$ can be constructed by combining the hyperplane representations of $\Lambda_{\mathrm{H}}^{\downarrow}(\boldsymbol{w}, \mathcal{L}_K)$ and $\Sigma(\boldsymbol{w})$ [61, 62, 76]. This combined representation also fully characterizes the non-convex set $\Lambda(\boldsymbol{w}, \mathcal{L}_K)$ defined in equation (26). Here, by combining two hyperplane representations, we simply mean to consider the collection of the inequalities arising from $\Lambda_{\mathrm{H}}^{\downarrow}(\boldsymbol{w}, \mathcal{L}_K)$ and $\Sigma(\boldsymbol{w})$. In general, this hyperplane representation of $\Lambda^{\downarrow}(\boldsymbol{w}, \mathcal{L}_K)$ will contain redundant inequalities, i.e. it will not be minimal, and a minimal hyperplane representation can be constructed.

Furthermore, if an inequality from the hyperplane representation of $\Sigma^{\downarrow}(\boldsymbol{w})$ is not facet-defining for $\Lambda^{\downarrow}(\boldsymbol{w}, \mathcal{L}_K)$, it can be tightened by shifting it until it becomes tangent to the boundary of $\Lambda^{\downarrow}(\boldsymbol{w}, \mathcal{L}_K)$. Mathematically, this process involves adjusting the right-hand side of the inequality $\boldsymbol{a}^{\mathrm{T}} \cdot \boldsymbol{\lambda}^{\downarrow} \leqslant b$, where $\boldsymbol{a}$ is the normal vector of the corresponding hyperplane $\mathcal{R}_i \equiv b - \boldsymbol{a}^{\mathrm{T}} \cdot \boldsymbol{\lambda}^{\downarrow} = 0$ and $b \in \mathbb{R}$. The quantity $\mathcal{R}_i \geqslant 0$, representing the difference between the right-hand side and left-hand side of the inequality, is commonly referred to as the residual.

This situation is illustrated in figure 2, where $\mathcal{R}_1$ and $\mathcal{R}_2$ represent two example residuals of the $\boldsymbol{w}$-ensemble N-representability constraints, expressed as $\mathcal{R}_i = b_i - \boldsymbol{a}_i^{\mathrm{T}} \cdot \boldsymbol{\lambda}^{\downarrow} \geqslant 0$ (see also section 4 for examples). In contrast, the tighter residual $\mathcal{R}_1'$ and its corresponding hyperplane (shown in blue), which is part of a hyperplane representation of $\Lambda_{\mathrm{H}}^{\downarrow}(\boldsymbol{w}, \mathcal{L}_K)$, is facet-defining, i.e. it is tight for the convex polytope $\Lambda^{\downarrow}(\boldsymbol{w}, \mathcal{L}_K)$ shown in gray. Similarly, the hyperplane described by $R_2 = 0$ is shifted until it touches the boundary of $\Lambda^{\downarrow}(\boldsymbol{w}, \mathcal{L}_K)$. In section 4, we will make use of this tightening to derive more restrictive bounds on the residuals of the $\boldsymbol{w}$-ensemble N-representability constraints.

Furthermore, since both $\Sigma(\boldsymbol{w}_{K^c})$ (29) and $\Sigma_{\mathrm{H}}^{\downarrow}(\{\boldsymbol{x}^{(i)\downarrow}\}_{i=1}^{|K|+1})$ in equation (28) are convex polytopes, the union over $\boldsymbol{x}^{(|K|+1)\downarrow} \equiv \widetilde{\boldsymbol{\lambda}}^{\downarrow} \in \Sigma(\boldsymbol{w}_{K^c})$ follows directly from a straightforward calculation. To highlight this key aspect and illustrate the calculation of $\Lambda^{\downarrow}(\boldsymbol{w}, \mathcal{L}_K)$, we consider the example of $r = 2$ nonzero weights w_i, $N = 2$, and $d = 3$. The sets $\Lambda(\boldsymbol{w}, \mathcal{L}_K)$ (green) and $\Lambda^{\downarrow}(\boldsymbol{w}, \mathcal{L}_K)$ (light green) for three different choices of $\boldsymbol{\lambda}^{(1)}$ are illustrated in figure 3. The original set $\Sigma(\boldsymbol{w})$ of admissible $\boldsymbol{w}$-ensemble natural occupation number vectors, without prior knowledge of parts of the ensemble, is shown in grey. Due to the normalization of the 1RDM to the total particle number $N = 2$, the third vector entry $\lambda_3 = 2 - \lambda_1 - \lambda_2$ is determined by the other two natural occupation numbers. Moreover, in appendix B, we explicitly derive the hyperplane representation of the convex set $\Lambda^{\downarrow}(\boldsymbol{w}, \mathcal{L}_K)$, illustrating the application of lemma 1.

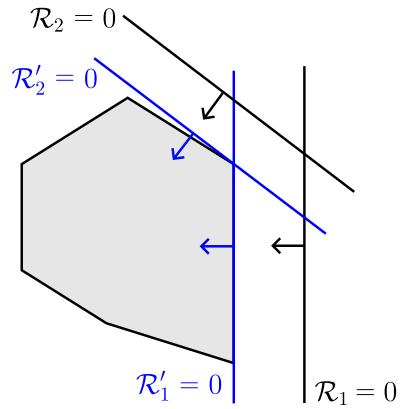

Figure 2. Schematic illustration of the tightening of $\boldsymbol{w}$-ensemble N-representability constraints for two inequalities in the hyperplane representation of $\Sigma(\boldsymbol{w})$. The vanishing residuals $R_j = 0$ (black) describing the two hyperplanes are shifted until they touch the boundary of the gray polytope leading to $R_j' = 0$ (blue). (See text for more explanations).

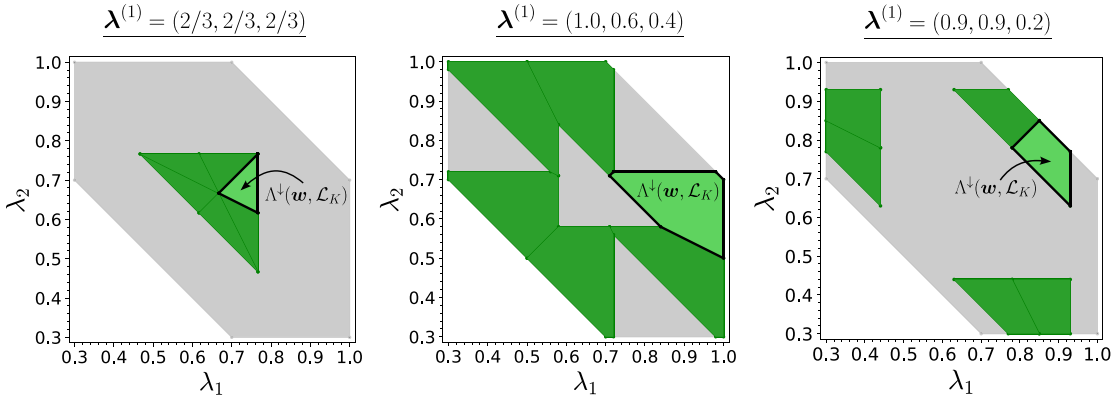

Figure 3. Illustration of the non-convex polytope $\Lambda(\boldsymbol{w}, \boldsymbol{\lambda}^{(1)})$ (green) and their dependence on $\boldsymbol{\lambda}^{(1)}$ for $N = 2, d = 3$, $\boldsymbol{w} = (0.7, 0.3, 0, \ldots)$ and three different choices of $\boldsymbol{\lambda}^{(1)}$. The set $\Lambda(\boldsymbol{w}, \boldsymbol{\lambda}^{(1)})$ follows from $\Lambda^{\downarrow}(\boldsymbol{w}, \boldsymbol{\lambda}^{(1)})$ (light green) by considering all possible permutations of $\boldsymbol{\lambda}^{\downarrow}$. The spectral polytope $\Sigma(\boldsymbol{w})$ is shown in gray and green. The value of $\lambda_3 = 2 - \lambda_1 - \lambda_2$ is fixed by the l^1-norm of $\boldsymbol{\lambda}$. (See text for more explanations.)

The in general non-convex set $\Lambda(\boldsymbol{w}, \mathcal{L}_K)$ follows from taking the orbit of $\Lambda^{\downarrow}(\boldsymbol{w}, \mathcal{L}_K)$ under the action of the symmetric group $\mathcal{S}_d$, i.e. by considering all possible permutations of the vector entries of any $\boldsymbol{\lambda} \in \Lambda^{\downarrow}(\boldsymbol{w}, \mathcal{L}_K)$. In particular, figure 3 stresses the dependence of the geometrical structure of the set $\Lambda(\boldsymbol{w}, \mathcal{L}_K)$ on the fixed natural occupation number vector $\boldsymbol{\lambda}^{(1)}$: for $\boldsymbol{\lambda}^{(1)} = (2/3, 2/3, 2/3)$ (left panel), i.e. the maximally mixed scenario, $\Lambda(\boldsymbol{w}, \mathcal{L}_K)$ is indeed a convex polytope. On the contrary, the center of $\Sigma(\boldsymbol{w})$ is not contained in $\Lambda(\boldsymbol{w}, \mathcal{L}_K)$ for less mixed $\boldsymbol{\lambda}^{(1)}$, as $\boldsymbol{\lambda}^{(1)} = (1, 0.6, 0.4), (0.9, 0.9, 0.2)$, in the middle and right panel. Moreover, also the number of facets and, thus, the number of facet-defining inequalities in a minimal hyperplane representation of $\Lambda^{\downarrow}(\boldsymbol{w}, \mathcal{L}_K)$ depends on $\boldsymbol{\lambda}^{(1)}$.

In addition to the refined $\boldsymbol{w}$-ensemble one-body N-representability problem treated above, where the full natural occupation vectors $\boldsymbol{\lambda}^{(i)}, i \in K$ are assumed known, one may also encounter cases in which only a subset of entries of each $\boldsymbol{\lambda}^{(i)}$ are fixed. This yields a further refinement of the N-representability problem. It can be addressed with the tools developed in this section, at the expense of a few additional technical conditions. For completeness, we present the required modifications for partially specified natural occupation numbers in appendix A.

3.2.3. Discussion

The derivation of the set $\Lambda^{\downarrow}(\boldsymbol{w}, \mathcal{L}_K)$ for $|K| = 1$ fixed natural occupation number vectors corresponds to the original Horn problem, which deals with the sum of two Hermitian matrices with fixed, decreasingly ordered vectors of eigenvalues, as explained in section 3.2.1. Even for $|K| = 1$, the number of linear constraints grows significantly with the dimension d of the one-particle Hilbert space $\mathcal{H}_1$. For example, for $d = 2$, there are six constraints, and for $d = 3$, there are already twelve, as discussed in [78, 79]. For generic $|K|$, the number of constraints increases rapidly [80]. Both $d = 2$ and $d = 3$ are far from typical

settings in quantum chemistry or physics, where d represents the dimension of the basis set or the number of lattice sites.

Furthermore, the hyperplane representations derived in [78, 80, 101, 102] are in general not minimal, meaning that some linear inequalities are redundant. A minimal set of linear inequalities for Horn's problem can be obtained using so-called honeycombs as explained in [106]. Moreover, due to the definition of $\Lambda_{\mathrm{H}}^{\downarrow}(\boldsymbol{w},\mathcal{L}_K)$, additional constraints are redundant, as we do not consider the generalized Horn problem for every set of Hermitian matrices. At the same time, this does not resolve the issue of determining the inequalities that solve Horn's problem for generic d in the first place. As discussed in the context of figure 3, the non-redundant linear constraints and, thus, the minimal hyperplane representation depend on $\boldsymbol{\lambda}^{(1)}$.

This leads to the following intermediate conclusion: By lemma 1 and theorem 2, we provide a concrete scheme that can be implemented numerically to derive the linear constraints characterizing the set $\Lambda^{\downarrow}(\boldsymbol{w},\mathcal{L}_K)$ and, consequently, $\Lambda(\boldsymbol{w},\mathcal{L}_K)$. These constraints can be easily checked for a given natural occupation number vector $\boldsymbol{\lambda}$. However, it is the non-convexity of $\Lambda(\boldsymbol{w},\mathcal{L}_K)$ that gives rise to the system-size dependent constraints from the generalized Horn problem in [80], going beyond the relaxed one-body $\boldsymbol{w}$-ensemble N-representability constraints, which characterize $\Sigma(\boldsymbol{w})$.

4. Improved bounds on residuals

In this section, we derive tighter bounds on the residuals of the $\boldsymbol{w}$-ensemble N-representability constraints that define the set $\Sigma(\boldsymbol{w})$ and present explicit examples of their application to small molecules. To this end, we begin with the simpler case of $r=2$ non-vanishing weights in the $\boldsymbol{w}$-ensemble in section 4.1. This serves as a primer for understanding the more general case of arbitrary $r\geqslant 3$, which is treated in section 4.2.

4.1. $\boldsymbol{w}$-ensembles with $r=2$

The knowledge about $\mathcal{L}_K$ directly impacts the residuals of the inequalities constituting the hyperplane representation of $\Sigma(\boldsymbol{w})$. Given $\Sigma(\boldsymbol{w})$, it is always possible to determine a (generally non-minimal) hyperplane representation of $\Lambda^{\downarrow}(\boldsymbol{w},\mathcal{L}_K)$ that includes hyperplanes with the same normal vectors as those in $\Sigma(\boldsymbol{w})$. Thus, $\mathcal{L}_K$ dictates which of the hyperplanes—from $\Sigma(\boldsymbol{w})$ or $\Lambda^{\downarrow}(\boldsymbol{w},\mathcal{L}_K)$ — is tight. Therefore, we obtain more restrictive residuals for the respective relaxed one-body $\boldsymbol{w}$-ensemble N-representability constraints. This procedure leads to a non-convex but easy-to-characterize outer approximation of $\Lambda(\boldsymbol{w},\mathcal{L}_K)$. In the following, we illustrate various theoretical concepts for $r=2$ as a proof-of-principle example. In fact, $r=2$ is particularly relevant for applications in functional theories, as it allows us to calculate the ground state energy and the ground state gap.

For $r=2$, the set $\Sigma(\boldsymbol{w})$ is defined by Coleman's one-body N-representability constraints [1] (see equation (C1) in appendix C), together with an additional $\boldsymbol{w}$-dependent constraint [61, 62, 76] whose residual is given by

$$\mathcal{R}_N(\boldsymbol{\lambda}) \equiv N-1+w-\sum_{i=1}^{N}\lambda_i^{\downarrow}\geqslant 0\,. \tag{35}$$

Moreover, we assume that $\mathcal{L}_K=(\boldsymbol{\lambda}^{(1)})$, while the result for $\mathcal{L}_K=(\boldsymbol{\lambda}^{(2)})$ follows analogously.

As a key result, we prove in appendix C that the sum of the k-largest natural occupation numbers λ_i is bounded from above by

$$\sum_{i=1}^{k}\lambda_i^{\downarrow}\leqslant \Omega(w,k,N,\mathcal{L}_K)=\begin{cases} w\sum_{i=1}^{k}\lambda_i^{(1)\downarrow}+(1-w)\min(k,N) & \text{if } k\neq N\\ \min\left(N-1+w, w\sum_{i=1}^{k}\lambda_i^{(1)\downarrow}+(1-w)N\right) & \text{if } k=N,\end{cases} \tag{36}$$

and from below by

$$\sum_{i=1}^{k}\lambda_i^{\downarrow}\geqslant N-w\left(N-\sum_{i=1}^{k}\lambda_i^{(1)\downarrow}\right)-(1-w)\,\chi_{N,d}^{(k)}\,, \tag{37}$$

where

$$\chi_{N,d}^{(k)}=\begin{cases} N & \text{if } d-1\geqslant N+k\,,\\ d-k-1 & \text{if } d-1<N+k\end{cases}\,. \tag{38}$$

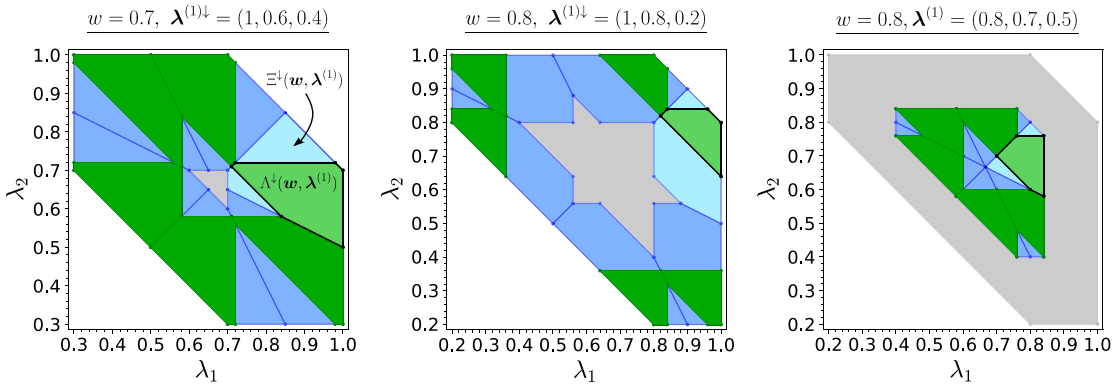

Figure 4. Illustration of the spectral polytopes $\Sigma(\boldsymbol{w}, \boldsymbol{\lambda}^{(1)})$ (green) and $\Xi(\boldsymbol{w}, \boldsymbol{\lambda}^{(1)})$ (blue and green) for $r = 2$ and three choices of $\boldsymbol{w}, \boldsymbol{\lambda}^{(1)}$. Both $\Lambda(\boldsymbol{w}, \boldsymbol{\lambda}^{(1)})$ and $\Xi(\boldsymbol{w}, \boldsymbol{\lambda}^{(1)})$ are subsets of the larger polytope $\Sigma(\boldsymbol{w})$ (grey, green and blue), with $\Lambda(\boldsymbol{w}, \boldsymbol{\lambda}^{(1)})$ contained within $\Xi(\boldsymbol{w}, \boldsymbol{\lambda}^{(1)})$.

The set of $\boldsymbol{\lambda}^{\downarrow}$ satisfying the constraints in equations (36) and (37) is denoted by $\Xi^{\downarrow}(\boldsymbol{w}, \boldsymbol{\lambda}^{(1)})$. Additionally, from the lower bounds in equation (37), we observe that the set $\Xi(\boldsymbol{w}, \boldsymbol{\lambda}^{(1)})$, obtained by considering all possible permutations of the spectra $\boldsymbol{\lambda} \in \Xi^{\downarrow}(\boldsymbol{w}, \boldsymbol{\lambda}^{(1)})$, is non-convex. At the same time, the hyperplane representation of $\Xi^{\downarrow}(\boldsymbol{w}, \boldsymbol{\lambda}^{(1)})$ in equations (37) and (36) is effectively independent of N, d. Furthermore, the spectral sets $\Xi(\boldsymbol{w}, \boldsymbol{\lambda}^{(1)})$, $\Lambda(\boldsymbol{w}, \boldsymbol{\lambda}^{(1)})$ satisfy the inclusion relations

$$\Lambda\left(\boldsymbol{w}, \boldsymbol{\lambda}^{(1)}\right) \subseteq \Xi\left(\boldsymbol{w}, \boldsymbol{\lambda}^{(1)}\right) \subseteq \Sigma(\boldsymbol{w})\,. \tag{39}$$

We illustrate the sets $\Xi(\boldsymbol{w}, \mathcal{L}_K)$ (blue) , $\Lambda(\boldsymbol{w}, \mathcal{L}_K)$ (green) and $\Sigma(\boldsymbol{w})$ (grey) for three different choices of $\boldsymbol{w}$ and $\boldsymbol{\lambda}^{(1)}$ in figure 4.

Through the knowledge of $\mathcal{L}_K$, the constraints in equations (36) and (37) further imply more restrictive constraints on the corresponding residuals of the relaxed $\boldsymbol{w}$-ensemble N-representability constraints for all $k \in \{1, \ldots, d-1\}$ as detailed in appendix C. In the following, we focus on the residual $\mathcal{R}_N(\boldsymbol{\lambda})$ in equation (35), as it corresponds to the single $\boldsymbol{w}$-ensemble one-body N-representability constraint that is more restrictive than Coleman's ensemble N-representability conditions. A brief calculation based on equation (36) (see appendix C) shows that the $\boldsymbol{w}$-dependent residual $\mathcal{R}_{\boldsymbol{w}}(\boldsymbol{\lambda})$ is bounded from below by

$$\mathcal{R}_N(\boldsymbol{\lambda}) \geqslant \max\left\{\mathcal{R}_{\min}^{\mathrm{triv}}, w\left(N - \sum_{i=1}^{N} \lambda_i^{(1)\downarrow}\right) - 1 + w\right\}, \tag{40}$$

where $\mathcal{R}_{\min}^{\mathrm{triv}} = 0$ represents the trivial lower bound, which holds independently of $\boldsymbol{\lambda}^{(1)}$. Equation (40) shows that the non-trivial lower bound becomes tighter as the l^1-norm $\|\boldsymbol{\lambda}^{(1)}\|_1$ deviates further from N. For ground states of physical systems, this means the non-trivial bound becomes tighter as the ground state becomes more correlated. In fact, a simple calculation shows that the new lower bound on $\mathcal{R}_N(\boldsymbol{\lambda})$ in equation (40) is more restrictive than the trivial lower bound $\mathcal{R}_N(\boldsymbol{\lambda}) \geqslant 0$ if

$$\sum_{i=1}^{N} \lambda_i^{(1)\downarrow} \leqslant N - \frac{1-w}{w}\,. \tag{41}$$

We illustrate this behavior using two chemical systems that exhibit strong correlation in certain parameter regimes: the hydrogen molecules H_2 and H_4, shown in figures 5 and 6, respectively. For both systems, we focus on the singlet sector and compute the ground and first excited states for various geometries using exact diagonalization in the cc-pvdz basis set. In the case of H_4, which consists of two H_2 dimers, the bond distance between the two hydrogen atoms in each dimer is fixed at $R_0 = 1.05\,\text{Å}$. The residual $\mathcal{R}_N(\boldsymbol{\lambda})$ is shown in red, and the lower bound from equation (40) is represented by the blue dashed lines. While H_2 shows strong static correlation in the dissociation limit, H_4 is strongly correlated when the distance R between the two H_2 dimers equals the fixed separation R_0. In particular, the new

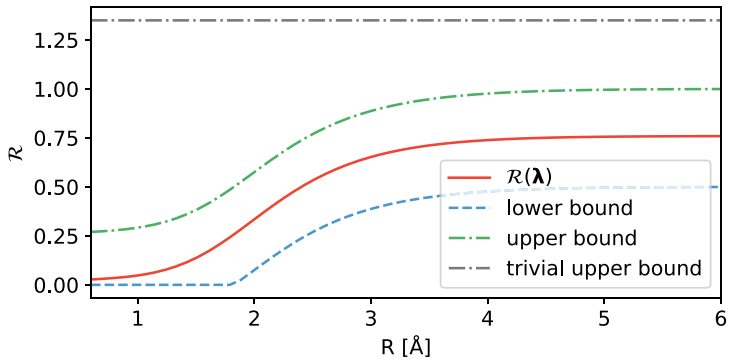

Figure 5. Illustration of the residual $\mathcal{R}_N(\boldsymbol{w})$ (red, solid) and its improved lower (blue, dashed) and upper (green, dashdotted) bound based on the knowledge of $\boldsymbol{\lambda}^{(1)}$ for H_2 in the singlet sector, $r = 2, w = 0.75$ in the cc-pvdz basis set. The trivial upper bound is shown in gray (dashdotted) and is always less restrictive than the new upper bound (see text for more details).

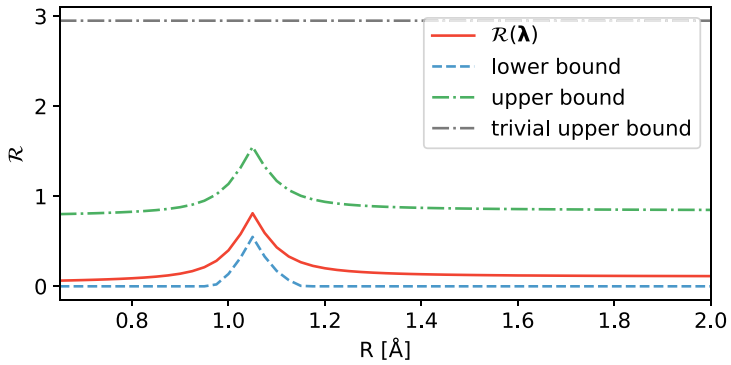

Figure 6. Illustration of the residual $\mathcal{R}_N(\boldsymbol{w})$ (red, solid) and its improved lower (blue, dashed) and upper (green, dashdotted) bound based on the information about the ground state natural occupation number vector $\boldsymbol{\lambda}^{(1)}$ for H_4 in the singlet sector, $r = 2, w = 0.75$ in the cc-pvdz basis set.

lower bound for the residual derived in equation (40) is indeed tighter than the trivial bound $\mathcal{R}^{\text{triv}}_{\text{min}} = 0$ in cases of strong correlation. The upper bounds on $\mathcal{R}_N(\boldsymbol{\lambda})$ will be discussed next.

The residual $\mathcal{R}_N(\boldsymbol{\lambda})$ is bounded from above by (see appendix C)

$$\mathcal{R}_N(\boldsymbol{\lambda}) \leqslant \min\left\{\mathcal{R}^{\text{triv}}_{\text{max}}, \mathcal{R}_{\text{max}}\left(\boldsymbol{\lambda}^{(1)}\right)\right\}, \tag{42}$$

where

$$\mathcal{R}_{\text{max}}\left(\boldsymbol{\lambda}^{(1)}\right) = \begin{cases} N-1+w\left(1-\sum_{i=1}^{N}\lambda_i^{(1)\downarrow}\right) & \text{if } d-1 \geqslant 2N, \\ d-2-N+w\left(2-d+2N-\sum_{i=1}^{N}\lambda_i^{(1)\downarrow}\right) & \text{if } d-1 < 2N \end{cases} \tag{43}$$

and the $\boldsymbol{w}$-dependent trivial upper bound $\mathcal{R}^{\text{triv}}_{\text{max}}$ on $\mathcal{R}(\boldsymbol{\lambda})$ in equation (42) is given by

$$\mathcal{R}^{\text{triv}}_{\text{max}} = w - 1 + N\left(1 - \frac{N}{d}\right). \tag{44}$$

As a consistency check, we observe that both the lower and upper bounds on $\mathcal{R}_N(\boldsymbol{\lambda})$ in equations (40) and (42) reduce to the correct value $N - \sum_{i=1}^{N}\lambda_i^{(1)\downarrow}$ in the limit $w \to 1$.

In contrast to the lower bound in equation (40), the non-trivial upper bound $\mathcal{R}_{\text{max}}(\boldsymbol{\lambda}^{(1)})$ becomes tighter as $\|\boldsymbol{\lambda}^{(1)}\|_1$ deviates less from N, i.e. the weaker the correlation in the ground state of a Hamiltonian. This behavior is further illustrated for H_2 and H_4 in figures 5 and 6, where both $\mathcal{R}^{\text{triv}}_{\text{max}}$ (grey, dash-dotted) and $\mathcal{R}_{\text{max}}(\boldsymbol{\lambda}^{(1)})$ (green, dash-dotted) are shown. In particular, we observe that $\mathcal{R}_{\text{max}}(\boldsymbol{\lambda}^{(1)})$ is more restrictive than $\mathcal{R}^{\text{triv}}_{\text{max}}$ over the entire parameter regime for varying R in both cases.

4.2. Generic $r \geqslant 3$

In this section, we outline the procedure for computing improved bounds on the residuals of the $\boldsymbol{w}$-ensemble N-representability constraints that characterize the set $\Sigma(\boldsymbol{w})$ for a general value of r. Specifically, for $r \geqslant 3$, all up to r natural occupation number vectors $\boldsymbol{\lambda}^{(i)}$ may be fixed, as discussed in section 3.2.

When $|K| = r-1$ natural occupation number vectors are fixed, we are left with only a single variable vector $\widetilde{\boldsymbol{\lambda}} \in \Sigma(\boldsymbol{w}_0)$. In this case, the derivation of the corresponding bounds on the residuals $\mathcal{R}_i$ proceeds analogously to the case $r=2$. However, when $|K| < r-1$, the union over all $\boldsymbol{x}^{(|K|+1)} \equiv \widetilde{\boldsymbol{\lambda}} \in \Sigma(\boldsymbol{w}_{K^c})$ in equation (28) reflects the fact that the remaining, non-fixed eigenvalue vectors arise from a $\boldsymbol{w}_{K^c}$-ensemble, as specified in equations (16) and (18).

As an illustrative example, we consider the case $r=3$, where $\boldsymbol{w} = (w_1, w_2, w_3, 0, \ldots)$ with $w_3 = 1 - w_1 - w_2$. The general case for $r \geqslant 3$ follows analogously. Since the case $|K| = 2$ corresponds directly to the $r=2$ scenario, we focus here on the case where only one, i.e. $|K| = 1$, natural occupation number vector is fixed. For concreteness, we assume this to be the one associated with the largest weight w_1. In this setting, we have $\boldsymbol{w}_{K^c} = (w_2, w_3, 0, \ldots)$ and $\widetilde{\boldsymbol{\lambda}} \in \Sigma(\boldsymbol{w}_{K^c})$. To compute the union over all $\widetilde{\boldsymbol{\lambda}} \in \Sigma(\boldsymbol{w}_{K^c})$, we must first characterize the set $\Sigma(\boldsymbol{w}_{K^c})$, which can be done analogously to the characterization of $\Sigma(\boldsymbol{w})$ presented in [61, 62]. In particular, a straightforward calculation shows that $\Sigma(\boldsymbol{w}_{K^c})$ corresponds to the permutohedron generated by the vertex

$$\boldsymbol{v} = \left(\underbrace{w_2 + w_3, \ldots, w_2 + w_3}_{N-1}, w_2, w_3, 0, \ldots \right) , \tag{45}$$

and thus given by

$$\Sigma(\boldsymbol{w}_{K^c}) = \mathrm{conv}\left(\{ \pi(\boldsymbol{v}) \,|\, \pi \in \mathcal{S}_d \} \right) . \tag{46}$$

In particular $\|\boldsymbol{v}\|_1 \neq N$, meaning that the $\boldsymbol{w}_{K^c}$ correspond to linear operators not normalized to unity (recall equations (16) and (17)).

For $r=3$, there are three non-trivial $\boldsymbol{w}$-dependent constraints characterizing the set $\Sigma(\boldsymbol{w})$ [61, 62, 76]. To illustrate the general procedure for deriving the refined bounds on the corresponding residuals, we pick as an example the residual $\mathcal{R}_N$ in equation (35), which is also present in the case of $r=2$. Then, following an argument analogous to the derivation of equation (36), the sum of the N largest eigenvalues is bounded from above by

$$\sum_{i=1}^{N} \lambda_i^{\downarrow} \leqslant \min \left(N - 1 + w_1, w_1 \sum_{i=1}^{N} \lambda_i^{(1)\downarrow} + (N-1)(w_2 + w_3) + w_2 \right) , \tag{47}$$

where, on the right-hand side, we have used the bound

$$\sum_{i=1}^{N} \widetilde{\lambda}_i^{\downarrow} \leqslant (N-1)(w_2 + w_3) + w_2 \tag{48}$$

which follows from Rado's theorem [107] and the hyperplane representation of $\Sigma(\boldsymbol{w}_{K^c})$ equation (46). The corresponding lower bound on $\sum_{i=1}^{N} \lambda_i^{\downarrow}$ can be derived in an analogous manner and, together with equation (47), yields improved bounds on $\mathcal{R}_N$ for $r=3$. Similarly, tighter bounds on the additional residuals constraining the set $\Sigma(\boldsymbol{w})$ can be obtained, though we leave the explicit calculations to the reader.

5. Convexification and application to lattice DFT

In this section, we discuss the convex hull of $\Xi(\boldsymbol{w}, \boldsymbol{\lambda}^{(1)})$. Moreover, we illustrate that the respective set characterizes the set of admissible densities in lattice DFT for $r=2$.

We first observe that by definition the convex hull of $\Xi(\boldsymbol{w}, \boldsymbol{\lambda}^{(1)})$,

$$\Sigma\left(\boldsymbol{w}, \boldsymbol{\lambda}^{(1)}\right) \equiv \mathrm{conv}\left(\Xi\left(\boldsymbol{w}, \boldsymbol{\lambda}^{(1)}\right) \right) , \tag{49}$$

is fully characterized by the upper bounds on the sum of the k-largest natural occupation numbers in equation (36) for all $k \in \{1, \ldots, d-1\}$.

The natural variable in lattice DFT is the lattice site occupation number vector $\boldsymbol{n} = \mathrm{diag}(\gamma)$ [108–116]. Therefore, the goal is to determine the set of $\boldsymbol{n}$ in ensemble lattice DFT for excited states (lattice ensemble DFT) [65–69, 71, 72, 74, 75] compatible with $\mathcal{L}_k$ for $r=2$. The Schur–Horn theorem [117, 118] implies that any lattice site occupation number vector $\boldsymbol{n}$ is majorized by the vector $\boldsymbol{\lambda}$ of eigenvalues of the 1RDM leading to

$$\sum_{i=1}^{k} n_i^{\downarrow} \leqslant \sum_{i=1}^{k} \lambda_i^{\downarrow} \leqslant \Omega\left(w,k,N,\mathcal{L}_K\right) \tag{50}$$

with $\Omega(w,k,N,\mathcal{L}_K)$ given by equation (36). It follows that for fixed $\boldsymbol{\lambda}^{(1)}$, the lattice site occupation number vector $\boldsymbol{n}$ in an ensemble DFT calculation for $r=2$ must be an element of the set $\Sigma(\boldsymbol{w},\boldsymbol{\lambda}^{(1)})$. To apply equation (50) in ensemble lattice ensemble DFT, one may exploit the knowledge of the ground state natural occupation number vector $\boldsymbol{\lambda}^{(1)}$ to restrict the set of admissible lattice site occupation number vectors $\boldsymbol{n}$ further. As a consequence of equation (42), equation (50) will be most restrictive if the ground state has strong static correlation. On the contrary, if applied to $\boldsymbol{\lambda}$ (and not $\boldsymbol{n}$), taking the convex hull constraints on the natural occupation number vectors in case the fully mixed 1RDM with spectrum $(N/d,\ldots,N/d)$ is inaccessible due to weak correlation in the N-particle state corresponding to $\boldsymbol{\lambda}^{(1)}$ (recall also section 4 and figures 5 and 6 for an illustration). In addition, one may exploit the freedom in choosing the weight vector $\boldsymbol{w}$ to make the set as restrictive as possible for a given $\boldsymbol{\lambda}^{(1)}$. For instance, the additional constraints in equation (50) will be particularly important when ground state functionals are employed to model also the excited states, as it is commonly the case in ensemble DFT.

We now provide a more detailed discussion of the geometric properties of $\Sigma(\boldsymbol{w},\boldsymbol{\lambda}^{(1)})$. Since $\Sigma(\boldsymbol{w})$ is a permutohedron for $r=2$, also the set $\Sigma(\boldsymbol{w},\boldsymbol{\lambda}^{(1)})$ is a permutohedron,

$$\Sigma\left(\boldsymbol{w},\boldsymbol{\lambda}^{(1)}\right) = \mathrm{conv}\left(\{\pi\left(\widetilde{\boldsymbol{\nu}}\right) \,|\, \pi \in \mathcal{S}_d\}\right). \tag{51}$$

The generating vertex $\widetilde{\boldsymbol{\nu}}$ of $\Sigma(\boldsymbol{w},\boldsymbol{\lambda}^{(1)})$ can be obtained from the hyperplane representation of $\Sigma(\boldsymbol{w},\boldsymbol{\lambda}^{(1)})$ through equation (36). This eventually leads to (see appendix D)

$$\begin{aligned}
\widetilde{\nu}_i &= w\lambda_i^{(1)\downarrow} + (1-w) \quad \text{for } 1 \leqslant i \leqslant N-1\,,\\
\widetilde{\nu}_N &= \min\left(w\lambda_N^{(1)\downarrow} + (1-w)\,, N-1+w-\sum_{j<N}\widetilde{\nu}_j\right),\\
\widetilde{\nu}_{N+1} &= w\lambda_{N+1}^{(1)\downarrow} + \widetilde{x}\\
\widetilde{\nu}_i &= w\lambda_i^{(1)\downarrow} \quad \forall i \in \{N+2,d\}\,,
\end{aligned} \tag{52}$$

where we defined

$$\widetilde{x} \equiv w\lambda_N^{(1)\downarrow} + (1-w) - \widetilde{\nu}_N \geqslant 0\,. \tag{53}$$

As a consistency check, we note that Rado's theorem [107] produces the inequalities in equation (36). Moreover, equation (36) reveals that unless all $(N-1)$ largest entries of $\boldsymbol{\lambda}^{(1)}$ equal one (recall figure 4 for $N=2$), the new exclusion principle constraints defining the spectral set $\boldsymbol{\lambda} \in \Sigma(\boldsymbol{w},\boldsymbol{\lambda}^{(1)})$ are always stricter than the $\boldsymbol{w}$-constraints that define $\Sigma(\boldsymbol{w})$.

Furthermore, using the hyperplane representation of the spectral set $\Sigma(\boldsymbol{w},\boldsymbol{\lambda}^{(1)})$, it follows from equation (49) that $\Sigma(\boldsymbol{w},\boldsymbol{\lambda}^{(1)})$ is given by the intersection.

$$\Sigma\left(\boldsymbol{w},\boldsymbol{\lambda}^{(1)}\right) \equiv \Sigma\left(\boldsymbol{w}\right) \cap \Sigma'\left(\boldsymbol{w},\boldsymbol{\lambda}^{(1)}\right), \tag{54}$$

where

$$\Sigma'\left(\boldsymbol{w},\boldsymbol{\lambda}^{(1)}\right) \equiv wP_{\boldsymbol{\lambda}^{(1)}} + (1-w)\,P_{\boldsymbol{\nu}^{\mathrm{HF}}} \tag{55}$$

with $\boldsymbol{\nu}^{\mathrm{HF}} = (1,\ldots,1,0,\ldots)$. Since $\Sigma'(\boldsymbol{w},\boldsymbol{\lambda}^{(1)})$ is convex as the Minkowski sum of two convex polytopes, $\Sigma(\boldsymbol{w},\boldsymbol{\lambda}^{(1)})$, being the intersection of two polytopes, is also convex in agreement with equations (49) and (54).

We illustrate equation (54) and (55) for $r=2, N=2, d=3$ and $\boldsymbol{\lambda}^{(1)} = (0.8,0.7,0.5), w=0.6$ in figure 7(see also the right panel of figure 4). The set $\Sigma'(\boldsymbol{w},\boldsymbol{\lambda}^{(1)})$ (blue) in equation (55) follows from

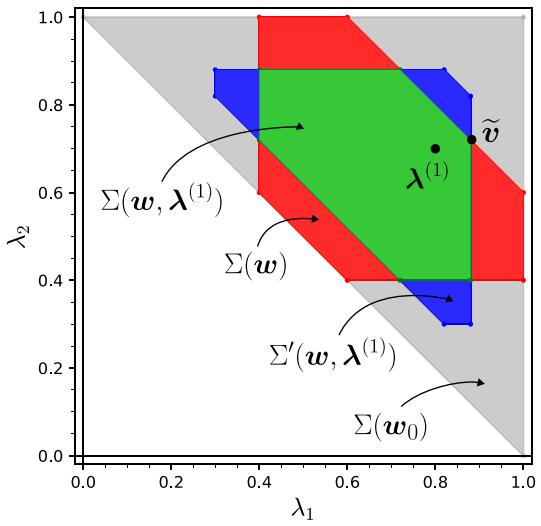

Figure 7. Illustration of the construction of the spectral set $\Sigma(\boldsymbol{w},\boldsymbol{\lambda}^{(1)})$ (49) (green) for $N=2, d=3$ such that $\lambda_3 = N-\lambda_1-\lambda_2$. The spectral set $\Sigma(\boldsymbol{w},\boldsymbol{\lambda}^{(1)})$ for fixed $\boldsymbol{\lambda}^{(1)}=(0.8,0.7,0.5)$ and $w=0.6$ follows from the intersection of $\Sigma'(\boldsymbol{w},\boldsymbol{\lambda}^{(1)})$ (blue) and $\Sigma(\boldsymbol{w})$ (red). The generating vertex of $\Sigma(\boldsymbol{w},\boldsymbol{\lambda}^{(1)})$ is denoted by $\widetilde{\boldsymbol{v}}$, and the grey polytope illustrates the Pauli simplex (see text for more explanations).

the Minkowski sum (i.e. element-wise sum of sets [119]) of the permutohedron of $\boldsymbol{\lambda}^{(1)}$ with the Pauli simplex $\Sigma(\boldsymbol{w}_0)$ (gray) (recall that $\boldsymbol{w}_0=(1,0,\ldots)$). According to equation (54), $\Sigma(\boldsymbol{w},\boldsymbol{\lambda}^{(1)})$ (green) eventually follows as the intersection of $\Sigma(\boldsymbol{w})$ (red) and $\Sigma'(\boldsymbol{w},\boldsymbol{\lambda}^{(1)})$ (blue).

6. Conclusions and outlook

In this work, we systematically addressed the refined N-representability problem for $\boldsymbol{w}$-ensemble 1RDMs, focusing on scenarios where partial information about the ensemble—such as full 1RDMs or their natural occupation numbers—is known *a priori*. Such situations naturally arise in $\boldsymbol{w}$-ensemble RDMFT calculations [61–64], where excited states are computed sequentially. Ensembles also emerge in systems with degenerate eigenstates and in open quantum systems. Extensions of the present framework to these broader contexts may be explored in future work.

We showed that incorporating known 1RDMs enables the formulation of a refined $\boldsymbol{w}$-ensemble one-body N-representability problem, which by construction imposes stricter constraints on the admissible set of 1RDMs than the original formulation [61–64]. However, this refined problem is inherently complex, as it is not a purely spectral problem and the admissible set of 1RDMs is non-convex. To address this, we introduced a hierarchy of systematic relaxations, ultimately yielding a spectral set defined by eigenvalue constraints that are practically characterizable. These developments provide a tractable and physically meaningful approach for incorporating refined N-representability constraints into functional theories.

We further investigated the geometric structure of the resulting non-convex spectral set and derived a hyperplane representation in terms of a finite number of linear inequalities on the natural occupation numbers. The physical significance of these system-size-independent constraints was supported by both analytic derivation and numerical illustration in molecular systems exhibiting varying degrees of correlation.

A key application of this work lies in $\boldsymbol{w}$-ensemble RDMFT [61–64] and ensemble DFT for excited states [65, 67–70, 73–75, 120, 121]. In $\boldsymbol{w}$-ensemble RDMFT, excited states are typically computed through a sequence of calculations with varying weight vectors $\boldsymbol{w}$, each containing an increasing number of non-zero components. At each step, the natural occupation number vectors of previously computed excited-state 1RDMs can be used to impose additional constraints, thereby restricting the optimization to a smaller, more physically relevant subset of ensemble 1RDMs. This is particularly advantageous when using approximate $\boldsymbol{w}$-ensemble RDMFT functionals, where such constraints may significantly enhance accuracy and stability. In particular, when computing energy gaps, this strategy allows one to leverage ground-state information already available from existing RDMFT functionals [23, 34, 40, 43, 45, 46, 48, 51, 52, 54, 56, 57].

Current ensemble DFT implementations often rely on ground-state functionals adapted to $\boldsymbol{w}$-ensembles due to practical limitations. The incorporation of additional information, such as natural occupation numbers from RDMFT or wave function methods, offers a path toward improved excited-state predictions within this framework.

These constraints can also be incorporated into variational two-electron RDM (2-RDM) methods [20, 21, 122–125] to provide approximate excited-state solutions. As in the case of the 1RDM theories, the constraints may permit a series of variational 2-RDM calculations with an increasing number of nonzero spectral weights w_i, from which an approximation to the excited states and their 2-RDMs can be computed.

Beyond applications in functional and variational methods, partial information about quantum ensembles—and the additional constraints it imposes on RDMs—may also prove valuable in reduced density matrix tomography [122–127] and in machine learning approaches for quantum systems [128, 129]. By integrating physically grounded constraints derived from ensemble theory, these data-driven or inference-based methods may achieve improved reliability, interpretability, and performance in future applications.

Finally, the framework for solving the refined $\boldsymbol{w}$-ensemble one-body N-representability problem can be extended beyond indistinguishable spinless fermions to bosons, spinful fermions, as well as distinguishable parties based on [63, 77, 130]. This enables applications to Rydberg-atom arrays, where (i) the full density matrix of few-atom subsets, and hence their single-site RDMs, can be reconstructed [131], and (ii) when coherences are inaccessible, only the diagonal elements of these 1RDMs are measured [132, 133]. Moreover, the convex hull of the set of admissible spectra discussed in section 5 can be applied directly to fermionic systems beyond lattice DFT whenever 1RDM information is available in a specified basis, such as the lattice-site representation in optical lattices [134, 135].

Data availability statement

All data that support the findings of this study are included within the article (and any supplementary files).

Acknowledgments

We acknowledge financial support from the U.S. National Science Foundation (NSF) Grant No. CHE-2155082 (D.M.), the German Research Foundation (Grant SCHI 1476/1-1) (J.L., C.S.), the U.S. NSF Graduate Research Fellowship Program under Grant No. 2140001 (I.A.), and the International Max Planck Research School for Quantum Science and Technology (IMPRS-QST) (J.L.). The Project/research is also part of the Munich Quantum Valley, which is supported by the Bavarian state government with funds from the Hightech Agenda Bayern Plus.

Appendix A. Incomplete knowledge about fixed natural occupation number vectors

In what follows, we consider a refinement of section 3.2 in which, for each $i \in K$ only a subset of entries of the natural occupation vector $\boldsymbol{\lambda}^{(i)} = (\mathcal{L}_K)_{\mu(i)}$ is known *a priori*. For instance, this setting may arise when only the largest few eigenvalues of some 1RDMs in the $\boldsymbol{w}$-ensemble are accessible. We focus on the additional constraints and steps required to solve the resulting N-representability problem under partial spectral information, and we highlight how these modifications differ from the original setting with fully specified natural occupation vectors as discussed in section 3.2. Each of the fixed $\lambda_j^{(i)}$ may be degenerate and we denote by m_i the number of distinct fixed $\lambda_j^{(i)}$ for each $\boldsymbol{\lambda}^{(i)}$. Then, we group the known natural occupation numbers with multiplicities $r_j^{(i)}$ as

$$\mathcal{M}^{(i)} \equiv \left\{ \left(\lambda_j^{(i)}, r_j^{(i)}\right) \right\}_{j=1}^{m_i}, \quad r_j^{(i)} \in \mathbb{N}, \quad \sum_{j=1}^{m_i} r_j^{(i)} = \left| J^{(i)} \right|, \tag{A1}$$

where $J^{(i)} \subseteq \{1, \ldots, d\}$ indexes the known entries. Crucially, we do not fix the positions of these values within $\boldsymbol{\lambda}^{(i)}$ as enforcing positions would require additional (more technical) ordering constraints and can be handled analogously if needed.

To describe admissible 1RDMs consistent with the partial data, we proceed in three steps: First, for each $i \in K$, we define the set of 1RDMs whose spectra contain the prescribed values with at least the indicated multiplicities:

$$\mathcal{X}^{(i)} \equiv \left\{ \gamma \in \mathcal{E}_N^1 \mid \exists \text{a set } \{P_j\}_{j=1}^{m_i} \text{of pairwise orthogonal projectors } P_j \text{ s.t. } \mathrm{rank}\,(P_j) \geqslant r_j^{(i)}, \left(\gamma - \lambda_j^{(i)} \mathbb{1}\right) P_j = 0 \, \forall j \right\}. \tag{A2}$$

Second, we impose that the weighted sum $\sum_{i\in K} w_i \gamma^{(i)}$ of the K components $\gamma^{(i)} \in \mathcal{X}^{(i)}, i \in K$ is an element of the set $\bar{\mathcal{E}}_N^1(\boldsymbol{w}_K)$, i.e. it represents a 1RDM that is compatible with an N-fermion quantum state whose spectrum is majorized by $\boldsymbol{w}_K$, which is the decreasingly ordered vector of weights w_i that correspond to the K fixed natural occupation number vectors (analogous to the definition of $\boldsymbol{w}_{K^c}$ in section 3.1) and takes the fixed. The set of all those 1RDMs is denoted by $\bar{\mathcal{E}}_N^1(\boldsymbol{w}_K, \mathcal{M}^{(i)})$. The set of natural occupation number vectors of 1RDMs $\gamma \in \bar{\mathcal{E}}_N^1(\boldsymbol{w}_K, \mathcal{M}^{(i)})$ is denoted by $\Sigma(\boldsymbol{w}_K, \mathcal{M}^{(i)})$. Third, for each eigenvalue vector $\boldsymbol{\lambda} \in \Sigma(\boldsymbol{w}_K, \mathcal{M}^{(i)})$, one returns to the generalized Horn's problem in section 3.2.1 and determines the set in equation (31). The union of these sets over all $\gamma \in \bar{\mathcal{E}}_N^1(\boldsymbol{w}_K)$ yields the solution to the refined $\boldsymbol{w}$-ensemble N-representability problem in which only selected entries of the $\boldsymbol{\lambda}^{(i)}$ are known *a priori*.

Appendix B. Refined non-relaxed w-ensemble N-representability constraints for $d = 3$ from Horn's problem

In this section, we show as an example for $d = 3$ how the refined $\boldsymbol{w}$-ensemble N-representability constraints characterizing the non-convex set $\Lambda(\boldsymbol{w}, \mathcal{L}_K)$ are obtained according to lemma 1. These will be the constraints that characterize the set $\Lambda^{\downarrow}(\boldsymbol{w}, \mathcal{L}_K)$ for the example in figure 3 in section 3.2.

We first recall Horn's problem discussed in section 3.2.1, i.e. the principal submatrix problem for three Hermitian matrices. Horn's problem asks the following question: given three decreasingly ordered vectors $\boldsymbol{x}^{\downarrow}, \boldsymbol{y}^{\downarrow}, \boldsymbol{z}^{\downarrow} \in \mathbb{R}^d$, do there exist three Hermitian matrices $X, Y, Z \in \mathbb{R}^{d\times d}$ such that $Z = X + Y$? The set of admissible $\boldsymbol{z}^{\downarrow}$ for fixed $\boldsymbol{x}^{\downarrow}, \boldsymbol{y}^{\downarrow}$ is a convex polytope denoted by $\Sigma_{\mathrm{H}}^{\downarrow}(\boldsymbol{x}, \boldsymbol{y})$, where the subscript H stands for Horn's problem. In our case the ensemble decomposition

$$\gamma = w\gamma^{(1)} + (1-w)\gamma^{(2)} \tag{B1}$$

is used to assign $Z \equiv \gamma, X = w\gamma^{(1)}, Y = (1-w)\gamma^{(2)}$, where only $\boldsymbol{x}^{\downarrow} \equiv \boldsymbol{\lambda}^{(1)\downarrow}$ is fixed. For $\boldsymbol{y}^{\downarrow} \equiv \boldsymbol{\lambda}^{(2)\downarrow}$ we consider all $\boldsymbol{\lambda}^{(2)\downarrow} \prec \boldsymbol{\nu}^{\mathrm{HF}}$ which are majorized by the Hartree–Fock natural occupation number vector $\boldsymbol{\nu}^{\mathrm{HF}} = (1, \ldots, 1, 0, \ldots, 0)$.

The goal of this section is to find the hyperplane representation of the set

$$\Lambda^{\downarrow}(\boldsymbol{w}, \mathcal{L}_K) = \Lambda_{\mathrm{H}}^{\downarrow}(\boldsymbol{w}, \mathcal{L}_K) \cap \Sigma(\boldsymbol{w}) \tag{B2}$$

of decreasingly ordered natural occupation number vectors $\boldsymbol{\lambda} \in \mathbb{R}^d$ as defined in equation (31) with $\Lambda_{\mathrm{H}}^{\downarrow}(\boldsymbol{w}, \mathcal{L}_K)$ given by equation (28) in the main text. A hyperplane representation of $\Sigma(\boldsymbol{w})$ is known from references [61, 62, 76]. To calculate the intersection of the two sets on the right hand-side of equation (B2), we have to determine (recall equation (28))

$$\Lambda_{\mathrm{H}}^{\downarrow}(\boldsymbol{w}, \mathcal{L}_K) \equiv \bigcup_{\boldsymbol{\lambda}^{(2)\downarrow} \in \Sigma^{\downarrow}(\boldsymbol{w}_0)} \Sigma_{\mathrm{H}}^{\downarrow}\left(\left\{ w_i \boldsymbol{\lambda}^{(i)\downarrow} \right\}_{i=1,2} \right). \tag{B3}$$

For $d = 3$ as discussed in this section, the solution to Horn's problem which characterizes the convex polytope $\Sigma_{\mathrm{H}}^{\downarrow}(\{w_i \boldsymbol{\lambda}^{(i)\downarrow}\}_{i=1,2})$ is given by the twelve inequalities [78, 79, 136]

$$\begin{aligned}
&\lambda_1^{\downarrow} \leqslant w\lambda_1^{(1)\downarrow} + (1-w)\lambda_1^{(2)\downarrow},\ \lambda_2^{\downarrow} \leqslant w\lambda_1^{(1)\downarrow} + (1-w)\lambda_2^{(2)\downarrow},\\
&\lambda_2^{\downarrow} \leqslant w\lambda_2^{(1)\downarrow} + (1-w)\lambda_1^{(2)\downarrow},\ \lambda_3^{\downarrow} \leqslant w\lambda_1^{(1)\downarrow} + (1-w)\lambda_3^{(2)\downarrow},\\
&\lambda_3^{\downarrow} \leqslant w\lambda_3^{(1)\downarrow} + (1-w)\lambda_1^{(2)\downarrow},\ \lambda_3^{\downarrow} \leqslant w\lambda_2^{(1)\downarrow} + (1-w)\lambda_2^{(2)\downarrow},\\
&\lambda_1^{\downarrow} + \lambda_2^{\downarrow} \leqslant w(\lambda_1^{(1)\downarrow} + \lambda_2^{(1)\downarrow}) + (1-w)(\lambda_1^{(2)\downarrow} + \lambda_2^{(2)\downarrow}),\\
&\lambda_1^{\downarrow} + \lambda_3^{\downarrow} \leqslant w(\lambda_1^{(1)\downarrow} + \lambda_3^{(1)\downarrow}) + (1-w)(\lambda_1^{(2)\downarrow} + \lambda_2^{(2)\downarrow}),\\
&\lambda_2^{\downarrow} + \lambda_3^{\downarrow} \leqslant w(\lambda_2^{(1)\downarrow} + \lambda_3^{(1)\downarrow}) + (1-w)(\lambda_1^{(1)\downarrow} + \lambda_2^{(1)\downarrow}),\\
&\lambda_1^{\downarrow} + \lambda_3^{\downarrow} \leqslant w(\lambda_1^{(1)\downarrow} + \lambda_2^{(1)\downarrow}) + (1-w)(\lambda_1^{(2)\downarrow} + \lambda_3^{(2)\downarrow}),\\
&\lambda_2^{\downarrow} + \lambda_3^{\downarrow} \leqslant w(\lambda_1^{(1)\downarrow} + \lambda_3^{(1)\downarrow}) + (1-w)(\lambda_2^{(2)\downarrow} + \lambda_3^{(2)\downarrow}),\\
&\lambda_2^{\downarrow} + \lambda_3^{\downarrow} \leqslant w(\lambda_1^{(1)\downarrow} + \lambda_3^{(1)\downarrow}) + (1-w)(\lambda_1^{(2)\downarrow} + \lambda_3^{(2)\downarrow}).
\end{aligned} \tag{B4}$$

Due to the linearity of ensemble one-body N-representability constraints, the union over all $\boldsymbol{\lambda}^{(2)\downarrow} \in \Sigma(\boldsymbol{w}_0)$ follows from a straightforward calculation for fixed value of the total particle number N.

Then, the hyperplane representation of the set $\Lambda^{\downarrow}_{\mathrm{H}}(\boldsymbol{w}, \mathcal{L}_K)$ in equation (B3) for $N=2$ follows as

$$\begin{aligned}
\lambda_1^{\downarrow} &\leqslant w\lambda_1^{(1)\downarrow} + 1 - w, \\
\lambda_2^{\downarrow} &\leqslant w\lambda_2^{(1)\downarrow} + 1 - w, \quad \lambda_3^{\downarrow} \leqslant w\lambda_1^{(1)\downarrow} + \frac{2(1-w)}{3}, \\
\lambda_3^{\downarrow} &\leqslant w\lambda_3^{(1)\downarrow} + 1 - w, \\
\lambda_1^{\downarrow} + \lambda_3^{\downarrow} &\leqslant w(\lambda_1^{(1)\downarrow} + \lambda_2^{(1)\downarrow}) + \frac{3(1-w)}{2}, \\
\lambda_2^{\downarrow} + \lambda_3^{\downarrow} &\leqslant w(\lambda_1^{(1)\downarrow} + \lambda_2^{(1)\downarrow}) + \frac{4(1-w)}{3}, \\
\lambda_2^{\downarrow} + \lambda_3^{\downarrow} &\leqslant w(\lambda_1^{(1)\downarrow} + \lambda_3^{(1)\downarrow}) + \frac{3(1-w)}{2}.
\end{aligned} \tag{B5}$$

Together with the relaxed $\boldsymbol{w}$-ensemble one-body N-representability constraints describing $\Sigma(\boldsymbol{w})$ the constraints in equation (B5) yield a hyperplane representation of the set $\Lambda^{\downarrow}(\boldsymbol{w}, \boldsymbol{\lambda}^{(1)})$. Moreover, a minimal hyperplane representation can be deduced based on $\boldsymbol{\lambda}^{(1)}$.

Appendix C. Derivation of the upper and lower bounds on the residuals for $r=2$

In this section, we derive the upper and lower bounds for the residuals of the relaxed one-body $\boldsymbol{w}$-ensemble N-representability constraints that characterize the spectral set $\Sigma(\boldsymbol{w})$ defined in equation (7).

We first recall that a hyperplane representation of $\Sigma(\boldsymbol{w})$ is given by [61, 62, 76]

$$\begin{aligned}
&\sum_{i=1}^{k} \lambda_i^{\downarrow} \leqslant k \quad \forall k \in \{1, \ldots, N-1\}, \\
&\sum_{i=1}^{N} \lambda_i^{\downarrow} \leqslant N - 1 + w \\
&\sum_{i=1}^{k} \lambda_i^{\downarrow} \leqslant N \quad \forall k \in \{N+1, \ldots, d-1\}, \\
&\sum_{i=1}^{d} \lambda_i^{\downarrow} = 1.
\end{aligned} \tag{C1}$$

Any linear inequality in equation (C1) can be written in the form $\boldsymbol{a}^{\mathrm{T}} \cdot \boldsymbol{\lambda}^{\downarrow} \leqslant b$. The residuals of these linear inequalities are defined as the difference between the right-hand side and the left-hand side, i.e. $\mathcal{R}_i(\boldsymbol{\lambda}) \equiv b - \boldsymbol{a}^{\mathrm{T}} \cdot \boldsymbol{\lambda}^{\downarrow} \geqslant 0$. For the single $\boldsymbol{w}$-dependent constraint in equation (C1) this leads to equation (35) in section 4.

Ky Fan showed in 1949, that a necessary linear inequality for the solution to Horn's problem is given by [79, 136] (translated into our setting)

$$\sum_{i=1}^{k} \lambda_i^{\downarrow} \leqslant \sum_{i=1}^{k} \left(w\lambda_i^{(1)\downarrow} + (1-w)\,\lambda_i^{(2)\downarrow} \right) \ \forall k \leqslant d. \tag{C2}$$

The above inequality immediately implies the sum of the k largest natural occupation numbers λ_i is bounded from below according to

$$\sum_{i=1}^{k} \lambda_i^{\downarrow} \geqslant w \sum_{i=1}^{k} \lambda_i^{(1)\downarrow} + (1-w)\min(k, N). \tag{C3}$$

In addition, we have the following upper bound for the smallest $d-k-1$ entries of $\boldsymbol{\lambda}$,

$$\sum_{i=k+1}^{d} \lambda_i^{\downarrow} \leqslant w \sum_{i=k+1}^{d} \lambda_i^{(1)\downarrow} + (1-w) \sum_{i=1}^{d-k-1} \lambda_i^{(2)\downarrow}. \tag{C4}$$

Due to the second term on the right hand-side we have to distinguish the two cases $d-1 \geqslant N+k$ and $d-1 < N+k$ for all $k \in \{1,\ldots,d-1\}$. Together with the normalizations $\|\boldsymbol{\lambda}^{(1)}\|_1 = \|\boldsymbol{\lambda}^{(2)}\|_1 = N$, we obtain

$$\sum_{i=k+1}^{d} \lambda_i^{\downarrow} \leqslant w \sum_{i=k+1}^{d} \lambda_i^{(1)\downarrow} + (1-w)\,\chi_{N,d}^{(k)}, \tag{C5}$$

where

$$\chi_{N,d}^{(k)} = \begin{cases} N & \text{if } d-1 \geqslant N+k, \\ d-k-1 & \text{if } d-1 < N+k \end{cases}. \tag{C6}$$

Therefore, it follows that the sum of the k-largest entries of $\boldsymbol{\lambda}$ is bounded from below by

$$\sum_{i=1}^{k} \lambda_i^{\downarrow} \geqslant N - w\left(N - \sum_{i=1}^{k} \lambda_i^{(1)\downarrow}\right) - (1-w)\,\chi_{N,d}^{(k)}, \tag{C7}$$

where we used the normalization $\sum_{i=1}^{d} \lambda_i = N$.

Therefore, the residuals $\mathcal{R}_k(\boldsymbol{\lambda})$ satisfy the lower bounds

$$\mathcal{R}_k(\boldsymbol{\lambda}) \geqslant \begin{cases} w\left(k - \sum_{i=1}^{k} \lambda_i^{(1)\downarrow}\right) \text{ if } k \in \{1,\ldots,N-1\}, \\ w - 1 + w\left(N - \sum_{i=1}^{k} \lambda_i^{(1)\downarrow}\right) \text{ if } k = N, \\ w\left(N - \sum_{i=1}^{k} \lambda_i^{(1)\downarrow}\right) \text{ if } k \in \{N+1,\ldots,d-1\} \end{cases}. \tag{C8}$$

Moreover, we obtain the following upper bounds

$$\mathcal{R}_k(\boldsymbol{\lambda}) \leqslant \begin{cases} k - N + w\left(N - \sum_{i=1}^{k} \lambda_i^{(1)\downarrow}\right) + (1-w)\,\chi_{N,d}^{(k)} & \text{if } k \in \{1,\ldots,N-1\}, \\ w\left(N - \sum_{i=1}^{k} \lambda_i^{(1)\downarrow}\right) + (1-w)\left(\chi_{N,d}^{(N)} - 1\right) & \text{if } k = N \\ w\left(N - \sum_{i=1}^{k} \lambda_i^{(1)\downarrow}\right) + (1-w)\,\chi_{N,d}^{(k)} & \text{if } k \in \{N+1,\ldots,d-1\} \end{cases}. \tag{C9}$$

Appendix D. Derivation of vertex representation of $\Sigma(w, \lambda^{(1)})$

In this section, we derive the vertex representation of $\Sigma(\boldsymbol{w},\boldsymbol{\lambda}^{(1)})$ for $r=2$ in section 5. From the hyperplane representation of the convex set $\Sigma(\boldsymbol{w},\boldsymbol{\lambda}^{(1)})$ in equation (49), we obtain that $\boldsymbol{\lambda} \in \Sigma(\boldsymbol{w},\boldsymbol{\lambda}^{(1)})$ if for all $1 \leqslant M \leqslant N-1$,

$$\sum_{i=1}^{M} \lambda_i^{\downarrow} \leqslant \min\left(M, w\sum_{i=1}^{M} \lambda_i^{(1)\downarrow} + M(1-w)\right). \tag{D1}$$

The smaller entry on the right hand-side in the above equation is always given by the second entry in the minimum, i.e. by $w\sum_{i=1}^{M} \lambda_i^{(1)\downarrow} + M(1-w)$. This implies that the $(N-1)$ largest entries of the generating vertex $\widetilde{\boldsymbol{\nu}}$ of the permutohedron $\Sigma(\boldsymbol{w},\boldsymbol{\lambda}^{(1)})$ are given by

$$\widetilde{\nu}_i = w\lambda_i^{(1)\downarrow} + (1-w) \quad \forall 1 \leqslant i \leqslant N-1. \tag{D2}$$

To derive the Nth largest entry of $\widetilde{\boldsymbol{\nu}}$ we use that

$$\sum_{i=1}^{N} \lambda_i^{\downarrow} \leqslant \min\left(N-1+w, w\sum_{i=1}^{N} \lambda_i^{(1)\downarrow} + N(1-w)\right), \tag{D3}$$

where the first entry of the minimum on the right hand-side arises from the hyperplane representation of $\Sigma(\boldsymbol{w})$. Using equation (D2) this implies that

$$\widetilde{\nu}_N = \min\left(w\lambda_N^{(1)\downarrow} + (1-w), N-1+w-\sum_{j<N} \widetilde{\nu}_j\right). \tag{D4}$$

Moreover, the hyperplane representation of $\Sigma(\boldsymbol{w},\boldsymbol{\lambda}^{(1)})$ implies that

$$\sum_{i=1}^{N+1}\lambda_i^{\downarrow} \leqslant \min\left(N, w\sum_{i=1}^{N+1}\lambda_i^{(1)\downarrow} + N(1-w)\right). \tag{D5}$$

Together with $\widetilde{\nu}_i$ for $i \leqslant N$, we obtain as an intermediate result that

$$\widetilde{\nu}_{N+1} = \min\left(N - \sum_{j<N+1}\widetilde{\nu}_j, w\left(\lambda_{N+1}^{(1)\downarrow} + \lambda_N^{(1)\downarrow}\right) + (1-w) - \widetilde{\nu}_N\right). \tag{D6}$$

Due to the normalization of $\boldsymbol{\lambda}^{(1)}$ to the total particle number, i.e. $\sum_{i=1}^{d}\lambda_i^{(1)\downarrow} = N$ it holds that

$$N - \sum_{j<N+1}\widetilde{\nu}_j \geqslant w\left(\lambda_{N+1}^{(1)\downarrow} + \lambda_N^{(1)\downarrow}\right) + (1-w) - \widetilde{\nu}_N. \tag{D7}$$

We then define the difference between $w\lambda_N^{(1)\downarrow} + (1-w)$ and $\widetilde{\nu}_N$ as

$$\widetilde{x} \equiv w\lambda_N^{(1)\downarrow} + (1-w) - \widetilde{\nu}_N \geqslant 0. \tag{D8}$$

Together with equation (D7) this implies that

$$\widetilde{\nu}_{N+1} = w\lambda_{N+1}^{(1)\downarrow} + \widetilde{x}. \tag{D9}$$

Moreover, it follows that

$$\widetilde{\nu}_i = w\lambda_i^{(1)\downarrow} \quad \forall N+2 \leqslant i \leqslant d. \tag{D10}$$

As a consistency check, we verify that the generating vertex $\widetilde{\boldsymbol{\nu}}$ is decreasingly ordered. The first N entries of $\widetilde{\boldsymbol{\nu}}$ are automatically decreasingly ordered. The same is true for the vector entries $\widetilde{\nu}_i \geqslant \widetilde{\nu}_j$ for $i<j, i,j \in \{N+1,\ldots,d\}$. Therefore, it remains to show that $\widetilde{\nu}_N \geqslant \widetilde{\nu}_{N+1}$. To this end, we first show that

$$\begin{aligned}\widetilde{x} &\leqslant w\sum_{i=1}^{N}\lambda_i^{(1)\downarrow} + (1-w) - Nw\\ &\leqslant 1-w,\end{aligned} \tag{D11}$$

where we used that

$$\widetilde{\nu}_N \geqslant wN - w\sum_{j=1}^{N-1}\lambda_j^{(1)\downarrow}. \tag{D12}$$

Using the upper bound on $\widetilde{x}$ we finally arrive at

$$\begin{aligned}\widetilde{\nu}_{N+1} - \widetilde{\nu}_N &\leqslant w\left(\lambda_{N+1}^{(1)\downarrow} - \lambda_N^{(1)\downarrow}\right) + \widetilde{x} - (1-w)\\ &\leqslant 0.\end{aligned} \tag{D13}$$

Thus, $\widetilde{\boldsymbol{\nu}}$ is indeed decreasingly ordered as required. This concludes the derivation of the vertex representation of $\Sigma(\boldsymbol{w},\boldsymbol{\lambda}^{(1)})$ for $r=2$.

ORCID iDs

Julia Liebert 0000-0002-4530-4900
Anna O Schouten 0000-0002-6425-5219
Irma Avdic 0000-0002-0731-9693
Christian Schilling 0000-0001-6781-4111
David A Mazziotti 0000-0002-9938-3886

References

[1] Coleman A J 1963 Structure of fermion density matrices *Rev. Mod. Phys.* **35** 668
[2] Garrod C and Percus J K 1964 Reduction of the N-particle variational problem *J. Math. Phys.* **5** 1756
[3] Kummer H 1967 n-representability problem for reduced density matrices *J. Math. Phys.* **8** 2063
[4] Erdahl R M 1978 Representability *Int. J. Quantum Chem.* **13** 697
[5] Coleman A J and Yukalov V 2000 *Reduced Density Matrices: Coulson's Challenge* (Springer) (available at: https://link.springer.com/book/9783540671480)
[6] Klyachko A 2006 Quantum marginal problem and N-representability *J. Phys.: Conf. Ser.* **36** 72
[7] Altunbulak M and Klyachko A 2008 The Pauli principle revisited *Commun. Math. Phys.* **282** 287
[8] Mazziotti D A 2012 Structure of fermionic density matrices: complete N-representability conditions *Phys. Rev. Lett.* **108** 263002
[9] Mazziotti D A 2012 Significant conditions for the two-electron reduced density matrix from the constructive solution of N representability *Phys. Rev. A* **85** 062507
[10] Maciazek T, Sawicki A, Gross D and Lopes A and Schilling C 2020 Implications of pinned occupation numbers for natural orbital expansions. II: Rigorous derivation and extension to non-fermionic systems *New J. Phys.* **22** 023002
[11] Schilling C, Benavides-Riveros C L, Lopes A, Maciazek T and Sawicki A 2020 Implications of pinned occupation numbers for natural orbital expansions: I. Generalizing the concept of active spaces *New J. Phys.* **22** 023001
[12] Mazziotti D A 2023 Quantum many-body theory from a solution of the N-representability problem *Phys. Rev. Lett.* **130** 153001
[13] Liu Y-K, Christandl M and Verstraete F 2007 Quantum computational complexity of the N-representability problem: QMA complete *Phys. Rev. Lett.* **98** 110503
[14] O'Gorman B, Irani S, Whitfield J and Fefferman B 2022 Intractability of electronic structure in a fixed basis *PRX Quantum* **3** 020322
[15] Klyachko A. 2004 Quantum marginal problem and representations of the symmetric group (arXiv:0409113)
[16] Schilling C, Gross D and Christandl M 2013 Pinning of fermionic occupation numbers *Phys. Rev. Lett.* **110** 040404
[17] Schilling C 2015 Quasipinning and its relevance for N-fermion quantum states *Phys. Rev. A* **91** 022105
[18] Schilling C, Benavides-Riveros C L and Vrana P 2017 Reconstructing quantum states from single-party information *Phys. Rev. A* **96** 052312
[19] Schilling C, Altunbulak M, Knecht S, Lopes A and Whitfield J D and Christandl M and Gross D and Reiher M 2018 Generalized Pauli constraints in small atoms *Phys. Rev. A* **97** 052503
[20] Mazziotti D A 2004 Realization of quantum chemistry without wave functions through first-order semidefinite programming *Phys. Rev. Lett.* **93** 213001
[21] Mazziotti D A 2011 Large-scale semidefinite programming for many-electron quantum mechanics *Phys. Rev. Lett.* **106** 083001
[22] Schilling C 2018 Communication: relating the pure and ensemble density matrix functional *J. Chem. Phys.* **149** 231102
[23] Piris M 2021 Global natural orbital functional: towards the complete description of the electron correlation *Phys. Rev. Lett.* **127** 233001
[24] Sager-Smith L M and Mazziotti D A 2022 Reducing the quantum many-electron problem to two electrons with machine learning *J. Am. Chem. Soc.* **144** 18959
[25] Sager L M, Schouten A O and Mazziotti D A 2022 Beginnings of exciton condensation in coronene analog of graphene double layer *J. Chem. Phys.* **156** 154702
[26] Jones G M, Li R R, DePrince A E I and Vogiatzis K D 2023 Data-driven refinement of electronic energies from two-electron reduced-density-matrix theory *J. Phys. Chem. Lett.* **14** 6377
[27] Eugene DePrince A III 2024 Variational determination of the two-electron reduced density matrix: a tutorial review *WIREs Comput Mol Sci.* **14** e1702
[28] Rubin N C, Babbush R and McClean J 2018 Application of fermionic marginal constraints to hybrid quantum algorithms *New J. Phys.* **20** 053020
[29] Smart S E and Mazziotti D A 2020 Efficient two-electron ansatz for benchmarking quantum chemistry on a quantum computer *Phys. Rev. Res.* **2** 023048
[30] Arute F *et al* 2020 Hartree-fock on a superconducting qubit quantum computer *Science* **369** 1084
[31] Raeber A E and Mazziotti D A 2020 Non-equilibrium steady state conductivity in cyclo[18]carbon and its boron nitride analogue *Phys. Chem. Chem. Phys.* **22** 23998
[32] Avdic I and Mazziotti D A 2024 Fewer measurements from shadow tomography with N-representability conditions *Phys. Rev. Lett.* **132** 220802
[33] Avdic I and Mazziotti D A 2024 Enhanced shadow tomography of molecular excited states via the enforcement of N-representability conditions by semidefinite programming *Phys. Rev. A* **110** 052407
[34] Gritsenko O, Pernal K and Baerends E J 2005 An improved density matrix functional by physically motivated repulsive corrections *J. Chem. Phys.* **122** 204102
[35] Pernal K and Giesbertz K J H 2016 *Reduced Density Matrix Functional Theory (Rdmft) and Linear Response Time-Dependent Rdmft (TD-Rdmft)* (*Density-Functional Methods for Excited States*) ed N Ferré, M Filatov and M Huix-Rotllant (Springer) p 125
[36] Kamil E, Schade R, Pruschke T and Blöchl P E 2016 Reduced density-matrix functionals applied to the Hubbard dimer *Phys. Rev. B* **93** 085141
[37] Schade R, Kamil E and Blöchl P 2017 Reduced density-matrix functionals from many-particle theory *Eur. Phys. J. Spec. Top.* **226** 2677
[38] Schade R and Blöchl P E 2018 Adaptive cluster approximation for reduced density-matrix functional theory *Phys. Rev. B* **97** 245131
[39] Benavides-Riveros C L and Marques M A L 2018 Static correlated functionals for reduced density matrix functional theory *Eur. Phys. J. B* **91** 133
[40] Piris M 2019 Natural orbital functional for multiplets *Phys. Rev. A* **100** 032508
[41] Mitxelena I, Piris M and Ugalde J M 2019 Chapter seven - advances in approximate natural orbital functional theory *State of The Art of Molecular Electronic Structure Computations: Correlation Methods, Basis Sets and More* (*Advances in Quantum Chemistry*) vol 79, ed L U Ancarani and P E Hoggan (Academic) p 155
[42] Schmidt J, Benavides-Riveros C L and Marques M A L 2019 Reduced density matrix functional theory for superconductors *Phys. Rev. B* **99** 224502

[43] Piris M and Mitxelena I 2021 DoNOF: an open-source implementation of natural-orbital-functional-based methods for quantum chemistry *Comput. Phys. Commun.* **259** 107651
[44] Di Sabatino S, Verdozzi C and Romaniello P 2021 Time dependent reduced density matrix functional theory at strong correlation: insights from a two-site Anderson impurity model *Phys. Chem. Chem. Phys.* **23** 16730
[45] Lemke Y, Kussmann J and Ochsenfeld C 2022 Efficient integral-direct methods for self-consistent reduced density matrix functional theory calculations on central and graphics processing units *J. Chem. Theory Comput.* **18** 4229
[46] Gibney D, Boyn J-N and Mazziotti D A 2022 Density functional theory transformed into a one-electron reduced-density-matrix functional theory for the capture of static correlation *J. Phys. Chem. Lett.* **13** 1382
[47] Mitxelena I and Piris M 2022 Benchmarking GNOF against FCI in challenging systems in one, two and three dimensions *J. Chem. Phys.* **156** 214102
[48] Senjean B, Yalouz S, Nakatani N and Fromager E 2022 Reduced density matrix functional theory from an ab initio seniority-zero wave function: exact and approximate formulations along adiabatic connection paths *Phys. Rev. A* **106** 032203
[49] Liebert J, Chaou A Y and Schilling C 2023 Refining and relating fundamentals of functional theory *J. Chem. Phys.* **158** 214108
[50] Sutter S M and Giesbertz K J H 2023 One-body reduced density-matrix functional theory for the canonical ensemble *Phys. Rev. A* **107** 022210
[51] Gibney D, Boyn J-N and Mazziotti D A 2023 Universal generalization of density functional theory for static correlation *Phys. Rev. Lett.* **131** 243003
[52] Gibney D, Boyn J-N and Mazziotti D A 2024 Enhancing density-functional theory for static correlation in large molecules *Phys. Rev. A* **110** L040802
[53] Benavides-Riveros C L, Wasak T and Recati A 2024 Extracting many-body quantum resources within one-body reduced density matrix functional theory *Phys. Rev. Res.* **6** L012052
[54] Vladaj M, Marécat Q, Senjean B and Saubanére M 2024 Variational minimization scheme for the one-particle reduced density matrix functional theory in the ensemble N-representability domain *J. Chem. Phys.* **161** 074105
[55] Cioslowski J and Strasburger K 2024 Constraints upon functionals of the 1-matrix, universal properties of natural orbitals and the fallacy of the Collins 'conjecture' *J. Phys. Chem. Lett.* **15** 1328
[56] Cartier N G and Giesbertz K J H 2024 Exploiting the Hessian for a better convergence of the SCF-RDMFT procedure *J. Chem. Theory Comput.* **20** 3669
[57] Yao Y-F and Su N Q 2024 Enhancing reduced density matrix functional theory calculations by coupling orbital and occupation optimizations *J. Phys. Chem. A.* **128** 7669–79
[58] Watanabe S 1939 Über die Anwendung thermodynamischer Begriffe auf den Normalzustand des Atomkerns *Z. Phys.* **113** 482–513
[59] Gross E K U, Oliveira L N and Kohn W 1988 Rayleigh-Ritz variational principle for ensembles of fractionally occupied states *Phys. Rev. A* **37** 2805
[60] Ding L, Hong C-L and Schilling C 2024 Ground and excited states from ensemble variational principles *Quantum* **8** 1525
[61] Schilling C and Pittalis S 2021 Ensemble reduced density matrix functional theory for excited states and hierarchical generalization of Pauli's exclusion principle *Phys. Rev. Lett.* **127** 023001
[62] Liebert J, Castillo F, Labbé J-P and Schilling C 2022 Foundation of one-particle reduced density matrix functional theory for excited states *J. Chem. Theory Comput.* **18** 124
[63] Liebert J and Schilling C 2023 An exact one-particle theory of bosonic excitations: from a generalized Hohenberg–Kohn theorem to convexified N-representability *New J. Phys.* **25** 013009
[64] Liebert J and Schilling C 2023 Deriving density-matrix functionals for excited states *SciPost Phys.* **14** 120
[65] Oliveira L N, Gross E K U and Kohn W 1988 Density-functional theory for ensembles of fractionally occupied states. II: Application to the He atom *Phys. Rev. A* **37** 2821
[66] Yang Z-h, Pribram-Jones A, Burke K and Ullrich C A 2017 Direct extraction of excitation energies from ensemble density-functional theory *Phys. Rev. Lett.* **119** 033003
[67] Fromager E 2020 Individual correlations in ensemble density functional theory: state- and density-driven decompositions without additional Kohn-Sham systems *Phys. Rev. Lett.* **124** 243001
[68] Loos P-F and Fromager E 2020 A weight-dependent local correlation density-functional approximation for ensembles *J. Chem. Phys.* **152** 214101
[69] Cernatic F, Senjean B, Robert V and Fromager E 2022 Ensemble density functional theory of neutral and charged excitations *Top. Curr. Chem.* **280** 4
[70] Gould T and Kronik L 2021 Ensemble generalized Kohn–Sham theory: the good, the bad and the ugly *J. Chem. Phys.* **154** 094125
[71] Yang Z-h 2021 Second-order perturbative correlation energy functional in the ensemble density-functional theory *Phys. Rev. A* **104** 052806
[72] Gould T, Kooi D P, Gori-Giorgi P and Pittalis S 2023 Electronic excited states in extreme limits via ensemble density functionals *Phys. Rev. Lett.* **130** 106401
[73] Giarrusso S and Loos P-F 2023 Exact excited-state functionals of the asymmetric Hubbard dimer *J. Phys. Chem. Lett.* **14** 8780
[74] Scott T R, Kozlowski J, Crisostomo S and Pribram-Jones A and Burke K 2024 Exact conditions for ensemble density functional theory *Phys. Rev. B* **109** 195120
[75] Cernatic F, Loos P-F, Senjean B and Fromager E 2024 Neutral electronic excitations and derivative discontinuities: an extended *n*-centered ensemble density functional theory perspective *Phys. Rev. B* **109** 235113
[76] Castillo F, Labbé J-P, Liebert J, Padrol A and Philippe E and Schilling C 2023 An effective solution to convex 1-body N-representability *Ann. Henri Poincaré* **24** 2241–321
[77] Liebert J, Castillo F, Labbé J-P, Maciazek M and Schilling C 2024 Solving one-body ensemble N-representability problems with spin (arXiv:2412.01805)
[78] Knutson A 2000 The symplectic and algebraic geometry of Horn's problem *Linear Algebra Appl.* **319** 61
[79] Bhatia R 2001 Linear algebra to quantum cohomology: the story of Alfred Horn's inequalities *Am. Math. Mon.* **108** 289
[80] Li C-K and Poon Y-T 2003 Principal submatrices of a Hermitian matrix *Linear Multilinear Algebra* **51** 199
[81] Eisert J, Tyc T, Rudolph T and Sanders B 2008 Gaussian quantum marginal problem *Nat. Commun.* **280** 263–80
[82] Walter M, Doran B, Gross D and Christandl M 2013 Entanglement polytopes: multiparticle entanglement from single-particle information *Science* **340** 1205
[83] Schilling C 2014 Quantum marginal problem and its physical relevance *PhD Thesis* ETH-Zürich (https://doi.org/10.3929/ethz-a-010139282)

[84] Christandl M, Doran B, Kousidis S and Walter M 2014 Eigenvalue distributions of reduced density matrices *Nat. Commun.* **332** 1
[85] Sawicki A, Oszmaniec M and Kuś M 2014 Convexity of momentum map, Morse index and quantum entanglement *Rev. Math. Phys.* **26** 1450004
[86] Wyderka N, Huber F and Gühne O 2017 Almost all four-particle pure states are determined by their two-body marginals *Phys. Rev. A* **96** 010102
[87] Bürgisser P, Christandl M, Mulmuley K D and Walter M 2017 Membership in moment polytopes is in NP and coNP *SIAM J. Comput.* **46** 972
[88] Maciazek T and Tsanov V 2017 Quantum marginals from pure doubly excited states *J. Phys. A: Math. Theor.* **50** 465304
[89] Christandl M, Şahinoğlu M and Walter M 2018 Recoupling coefficients and quantum entropies *Ann. Henri Poincaré* **19** 385–410
[90] Yu X-D, Simnacher T, Wyderka N and Nguyen H C and Gühne O 2021 A complete hierarchy for the pure state marginal problem in quantum mechanics *Nat. Commun.* **12** 1012
[91] Haapasalo E, Kraft T, Miklin N and Uola R 2021 Quantum marginal problem and incompatibility *Quantum* **5** 476
[92] Hsieh C-Y, Lostaglio M and Acín A 2022 Quantum channel marginal problem *Phys. Rev. Res.* **4** 013249
[93] Gühne O, Haapasalo E, Kraft T and Pellonpää J-P and Uola R 2023 Colloquium: incompatible measurements in quantum information science *Rev. Mod. Phys.* **95** 011003
[94] Klyachko A 2009 The Pauli exclusion principle and beyond (arXiv:0904.2009)
[95] Reuvers R 2021 Generalized Pauli constraints in large systems: the Pauli principle dominates *J. Math. Phys.* **62** 032204
[96] Alberti P and Uhlmann A 1982 *Stochasticity and Partial Order: Doubly Stochastic Maps and Unitary Mixing* (*Mathematics and Its Applications*) (Springer) (available at: https://books.google.co.uk/books?id=cVHTS7cjkqsC)
[97] Valone S M 1980 Consequences of extending 1-matrix energy functionals from pure–state representable to all ensemble representable 1-matrices *J. Chem. Phys.* **73** 1344
[98] Lieb E H 1983 Density functionals for Coulomb systems *Int. J. Quantum Chem.* **24** 243
[99] Theophilou A K 1979 The energy density functional formalism for excited states *J. Phys. C: Solid State Phys.* **12** 5419
[100] Rockafellar R T 1997 *Convex Analysis* (Princeton university press) (available at: https://press.princeton.edu/titles/1815.html)
[101] Klyachko A 1998 Stable bundles, representation theory and Hermitian operators *Sel. Math., New Ser.* **4** 419
[102] Knutson A and Tao T 1999 The honeycomb model of $GL_N(\mathbb{C})$ tensor products I: proof of the saturation conjecture *J. Am. Math. Soc.* **12** 1055
[103] Kirwan F 1984 Convexity properties of the moment mapping, III *Invent. Math.* **77** 547–52
[104] Guillemin V 1994 *Moment Maps and Combinatorial Invariants of Hamiltonian Tn-Spaces* (Birkhäuser) (https://doi.org/10.1007/978-1-4612-0269-1)
[105] The Sage Developers SageMath, the Sage mathematics software system (version x.y.z) (available at: www.sagemath.org)
[106] Knutson A, Tao T and Woodward C 2004 The honeycomb model of $GL_N(\mathbb{C})$ tensor products II: puzzles determine facets of the Littlewood-Richardson cone *J. Am. Math. Soc.* **17** 19
[107] Rado R 1952 An inequality *J. Lond. Math. Soc.* **1** 1
[108] Gunnarsson O and Schönhammer K 1986 Density-functional treatment of an exactly solvable semiconductor model *Phys. Rev. Lett.* **56** 1968
[109] Schönhammer K, Gunnarsson O and Noack R M 1995 Density-functional theory on a lattice: comparison with exact numerical results for a model with strongly correlated electrons *Phys. Rev. B* **52** 2504
[110] Ijäs M and Harju A 2010 Lattice density-functional theory on graphene *Phys. Rev. B* **82** 235111
[111] Xianlong G, Chen A-H, Tokatly I V and Kurth S 2012 Lattice density functional theory at finite temperature with strongly density-dependent exchange-correlation potentials *Phys. Rev. B* **86** 235139
[112] Saubanère M and Pastor G M 2014 Lattice density-functional theory of the attractive Hubbard model *Phys. Rev. B* **90** 125128
[113] Coe J P 2019 Lattice density-functional theory for quantum chemistry *Phys. Rev. B* **99** 165118
[114] Penz M and van Leeuwen R 2021 Density-functional theory on graphs *J. Chem. Phys.* **155** 244111
[115] Penz M and van Leeuwen R 2023 Geometry of degeneracy in potential and density space *Quantum* **7** 918
[116] Penz M and van Leeuwen R 2024 Geometrical perspective on spin–lattice density-functional theory *J. Chem. Phys.* **161** 150901
[117] Schur I 1923 Über eine Klasse von Mittelbildungen mit Anwendungen die Determinanten-Theorie *Sitzungsber. Berl. Math. Ges.* **22** 9
[118] Horn A 1954 Doubly stochastic matrices and the diagonal of a rotation matrix *Am. J. Math.* **76** 620
[119] Ziegler G M 1994 *Lectures on Polytopes* (Springer)
[120] Gross E K U, Oliveira L N and Kohn W 1988 Density-functional theory for ensembles of fractionally occupied states. I: basic formalism *Phys. Rev. A* **37** 2809
[121] Fromager E 2025 Ensemble density functional theory of ground and excited energy levels *J. Phys. Chem. A* **129** 1143
[122] Mazziotti D A 2020 Dual-cone variational calculation of the two-electron reduced density matrix *Phys. Rev. A* **102** 052819
[123] Knight M J, Quiney H M and Martin A M 2022 Reduced density matrix approach to ultracold few-fermion systems in one dimension *New J. Phys.* **24** 053004
[124] Schouten A O, Klevens J E, Sager-Smith L M, Xie J, Anderson J S and Mazziotti D A 2023 Potential for exciton condensation in a highly conductive amorphous polymer *Phys. Rev. Mater.* **7** 045001
[125] Xie J *et al* 2022 Intrinsic glassy-metallic transport in an amorphous coordination polymer *Nature* **611** 479
[126] Xin T, Lu D, Klassen J, Yu N, Ji Z, Chen J, Ma X, Long G, Zeng B and Laflamme R 2017 Quantum state tomography via reduced density matrices *Phys. Rev. Lett.* **118** 020401
[127] Zhao A, Rubin N C and Miyake A 2021 Fermionic partial tomography via classical shadows *Phys. Rev. Lett.* **127** 110504
[128] Shao X, Paetow L, Tuckerman M E and Pavanello M 2023 Machine learning electronic structure methods based on the one-electron reduced density matrix *Nat. Commun.* **14** 6281
[129] Hazra S, Patil U and Sanvito S 2024 Predicting the one-particle density matrix with machine learning *J. Chem. Theory Comput.* **20** 4569
[130] Castillo F and Labbé J-P 2025 Lineup polytopes of products of simplices *Ann. Inst. Henri Poincaré Comb. Phys. Interact.* **12** 787
[131] Kim K and Ahn J 2023 Quantum tomography of Rydberg atom graphs by configurable ancillas *PRX Quantum* **4** 020316
[132] Browaeys A and Lahaye T 2020 Many-body physics with individually controlled Rydberg atoms *Nat. Phys.* **16** 132
[133] Semeghini G *et al* 2021 Probing topological spin liquids on a programmable quantum simulator *Science* **374** 1242
[134] Bakr W S, Gillen J I, Peng A and Fölling S and Greiner M 2009 A quantum gas microscope for detecting single atoms in a Hubbard-regime optical lattice *Nature* **462** 74
[135] Gross C and Bloch I 2017 Quantum simulations with ultracold atoms in optical lattices *Science* **357** 995
[136] Fulton W 2000 Eigenvalues, invariant factors, highest weights and Schubert calculus *Bull. Am. Math. Soc.* **37** 209